

Probabilistic classification of soils based on Local Average Subdivision method and CPT data

Additional thesis (10 ECTs)

Sijun Zeng

MSc in Geo-Engineering

5561213

Supervisors:

Dr. Divya Varkey

Dr. ir. Bram van den Eijnden

Prof. Dr. Michael Hicks

October 7, 2022



Contents

Abstract	4
1. Introduction	5
1.1 General background	5
1.2 Scope of this study	5
2. Literature Review	6
2.1 Cone Penetration Test	6
2.2 Soil Classification Method	6
2.3 Random field	6
3. Methodology	8
3.1 Soil Classification method based on CPT	8
3.2 Conditional random field generator based on LAS and Kriging	10
3.2.1 Random field generator based on Local Average Subdivision	10
3.2.2 Condition random field generator based on LAS and Kriging interpolation .	13
3.3 Input parameter identification	14
3.4 Automatic data processing	15
4. Illustrative example	19
4.1 Input determination	19
4.2 Results and analysis	20
4.2.1 Most probable result for classifications and its uncertainty	20
4.2.2 Comparison between conditional and unconditional random field generator	21
4.2.3 Convergence in the unconditional random field	23
5. Case Study	27
5.1 Background	27
5.2 Input data	28
5.3 Results and analysis	31
5.3.1 Most probable result for classifications and its uncertainty	31
5.3.2 Comparison between conditional and unconditional random field generator	32
5.4 Influence of one less CPT	33
6. Limitation and optimization	37
6.1 Uncertainty in soil classification model	37
6.2 Combination with boundary based model	38

7. Conclusion	39
Reference	40
Appendices: Python Codes	43

Abstract

A random field generator based on Local Average Subdivision (LAS) method is proposed in this study in order to achieve probabilistic soil classification and quantify the uncertainty of the generated most probable geological cross section. CPT data and Robertson's soil classification chart (1990) are adopted to classify the soil. The sole application of LAS makes the random field unconditional, which has been improved to conditional random field generator by using Kriging interpolation. Both unconditional and conditional generator are tested in an illustrative example and the results indicate that the improvement from unconditional to conditional random field reduces the uncertainty of the most probable result of classifications and the classifications in the unconditional random field will converge if there are enough realizations. Additionally, the conditional random field generator is further applied in a case with three conducted CPTs, which build up a domain with very large scale of fluctuations. It's found that the uncertainty of the generated most probable result of classifications is pretty low so it's speculated that the proposed generator can be best applied in a large scale of fluctuation scenario. Another finding in the case study is that the proposed random field generator can be used to verify the reliability of conducted CPTs.

1. Introduction

1.1 General background

The subsurface soil stratigraphy, which constitutes a part of site characterization, plays an important role in the construction works and geotechnical structures (Wang, Wang & Liang, 2017; Clayton, 2001). As for how to develop a underground geological cross-section, traditionally people simply draw straight lines to connect the boundaries of the same soil types between two adjacent site investigation (e.g. CPT, borehole, etc.). This traditional method has been used for a long time but it can only be applied when site has relatively simple geology or when extensive ground investigations are available (Shi & Wang, 2021) because it actually ignores the possible inconsistency of the soil boundaries and reduces the uncertainty of soil classifications arbitrarily. The application of such a method in real engineering cases may lead to many problems. So how to obtain a geological cross section approaching to the real in-situ condition under the circumstance that the site investigations are sparse and the underground geological situation is complicated becomes the research question for this project.

The solution, also the research objectivity of this project, to the aforementioned problem is to carry on probabilistic soil classifications and find the geological cross section in a stochastic way. This method offers a great opportunity to capture the soil inherent variability by random field and infer the most probable result of classifications, especially the classifications at unsampled locations. Moreover the uncertainty can be quantified, which means that the uncertainty of the most probable result can also be obtained. In all, in this way the geological cross section can be inferred in a stochastic way instead of a deterministic way.

Many probabilistic approaches have been developed such as random field and machine learning methods (Shi & Wang, 2021a; Shi & Wang, 2021b; Hu & Wang, 2020; Chessa, 2006). Specifically in this study, how to achieve the probabilistic analysis has been divided into two parts: the soil classifications based on CPT data and the random field generator based on Local Average Subdivision method and Kriging interpolation.

1.2 Scope of this study

In order to deal with stochastic soil stratigraphy, there are two key parts: soil classification model and random field generator. In this study, for the former one, Robertson's CPT classification method (Robertson, 1990) is adopted and it will be elaborated in Section 3.1. For the latter one, conditional random field generator based on Local Average Subdivision and Kriging Interpolation is adopted, which will be elaborated in Section 3.2.1 (LAS) and Section 3.2.2 (Kriging interpolation). The most probable results for classifications and their uncertainties, as well as some other post-analysis will be elaborated in Chapter 4 and Chapter 5, respectively for an illustrative example and a real case.

There are many other methods to achieve soil classification besides CPT classification and there are many other methods to generate random field no matter it is stationary or non-stationary. This study can function as a contrast example for researchers who want to investigate in and find out the most accurate and convenient way to achieve probabilistic soil classifications.

2. Literature Review

2.1 Cone Penetration Test

The site investigation method used on this study is Cone Penetration Test (CPT). The test method consists of pushing an instrumented cone, with the tip facing down, into the ground at a controlled rate (controlled between 1.5 -2.5 cm/s accepted) ("Cone penetration test - Wikipedia", 2022). It is a widely used in-situ test to identify soil types. There are a couple of advantages of such a test: providing accurate and continuous profiles (Ramsey, 2010), being fast, repeatable and economical (Robertson, 2010); the data obtained from CPT being able to interpret soil properties based on some empirical relations (e.g. shear wave velocity, undrained shear strength, particle size and hydraulic conductivity; McGann, Bradley, Taylor, Wotherspoon & Cubrinovski, 2015; Anagnostopoulos, Koukis, Sabatakakis, & Tsiambaos, 2003; Tillmann et al., 2008). The disadvantage exists in terms of only being applicable for shallow subsurface, not considering cyclic loading conditions, etc. (Ramsey, 2010). What is obtained from CPT and how to use specifically in this study will be elaborated in Section 3.1.

2.2 Soil Classification Method

Soil classification has been important in geotechnical engineering field for a long time and there are many methods well developed. In the following there are some classical soil classification methods chosen to display: American Association of State Highway and Transportation Officials (AASHTO) soil classification system which applies sieve analysis, plastic limit and liquid limit to classify; Unified Soil Classification System (USCS) which applies texture and grain size to classify; The United States Department of Agriculture (USDA) method textural soil classification method which also applies soil textures to classify; soil behavior type (Robertson, 1990) and soil behavior type index I_c (Robertson & Wride, 1998) which applies normalized cone resistance and friction ratio to classify.

In order to obtain necessary parameters for those classification methods, there are various in-situ tests and experimental tests developed. For AASHTO soil classification, sieve analysis and Atterberg Limit Test are needed. For soil behavior type and soil behavior type index I_c , CPT or flat plate dilatometer test (Robertson, 2015) are needed. In addition, some methods only require people to identify visually, like UCSC and USDA method, needing people to classify the soils by observing soils' texture.

2.3 Random field

Random field originates from mathematics and physics and it has a wide range of applications. Generally it can be defined as the representation of the joint probability distribution for a set of random variables (Hernández-Lemus, 2021). In this study, the random field can be simply understood as a domain where there are random variables generated in each element for each realization. One realization means the generation of a random property field and subsequent analysis of the problem (Hicks, 2009).

As for how to generate random field, there are various ways. In general it can be divided into two types: stationary (Gaussian) random field, which is commonly used and non-stationary (non-Gaussian) random field. For stationary method, there are Fast Fourier Method, Turning Bands Method, Spectral method, Matrix decomposition method, Karhunen-Loeve expansion, Moving average, Sequential simulation and Local Average Subdivision method (Liu, Li, Sun & Yu, 2019). Compared to other methods, the Local Average Subdivision, which is adopted in this study, has the advantage that it is straightforward and fast (Fenton & Griffiths, 2007). Detailed information about LAS will be shown in Section 3.2.1. In non-stationary random field, the statistics of data points (e.g. mean, standard deviation) change in temporal dimension or in space dimension. This may be an advantage, especially when analyzing CPT data because CPT data is strictly non-stationary (Jamshidi & Kamyab, 2015). It has an inherent depth trend. In non-stationary random field all the data doesn't have to be detrended which conforms with reality and avoid potential inaccuracies. Nowadays, there are a large number of investigations in non-stationary random field (Griffiths, Huang & Fenton, 2015; Montoya-Noguera, Zhao, Hu, Wang, & Phoon, 2019; Hu & Wang, 2020), which shows the potential to become a trending topic.

There is an overview of a non-stationary generator, Bayesian compressive sampling Karhunen-Loève (BCS-KL) generator, proposed by Hu & Wang (2020), which may be helpful for researchers who are interested in it. This generator is based on a novel sampling concept called compressive sampling/sensing (CS): A certain signal or image (like the qt and Fr which are investigated in this study) can be reconstructed from sparse measurements on that signal or image. The reconstruction is based on the fact that many natural signals are compressible. In other words, a signal/image can be estimated by a limited number of weight coefficients multiplied by respective basis functions like wavelet functions and cosine functions. Specifically it is achieved by the following equations:

$$F = \sum_{t=1}^{N_{x1} \times N_{x2}} B_t^{2D} w_t^{2D} \quad (1)$$

$$Y = \psi_{x1} F \psi_{x2} \quad (2)$$

where F is the 2D signal/image to be reconstructed, B_t^{2D} is the t -th 2D basis function; w_t^{2D} is the weight coefficients corresponding to B_t^{2D} ; Y is a sub-matrix of F constituted by sparse measurements. In this case, Y can be simply understood as a 2D matrix which consists of 1D conducted CPTs. Detailed mathematical derivation can be viewed in Hu and Wang's paper. One highlight can be seen in those equations that this generator bypasses the difficulty to connect the conducted CPT to the input parameters used in the random field. The measurements are directly used as input for reconstruction. How to solve such a difficulty in this study is shown in Section 3.3 but no matter how subtle the solution is, it is not as direct as the BCS-KL generator and more procedures mean more inaccuracies. So that's the most valuable point worth researching. In addition, the 2D matrix F can automatically remain the anisotropic/isotropic trait.

3. Methodology

3.1 Soil Classification method based on CPT

In this study, Robertson's CPT classification chart (1990) is adopted. There are some empirical relations between the soil behavior types and normalized friction ratio (F_r) and normalized cone resistance (Q_t), which can be seen in Fig. 1. The number 1 to 9 in Fig. 1 refers to the soil behavior type, and Fig. 2 illustrates detailed descriptions. It's worthy noticing that F_r and Q_t can not be directly measured from CPT but can be indirectly calculated by some parameters measured by CPT. The relationship is shown below.

$$Q_t = \frac{q_t - \sigma_{v0}}{\sigma'_{v0}} \quad (3)$$

$$F_r = \frac{f_s}{q_t - \sigma_{v0}} \times 100 \quad (4)$$

Where,

$q_t = q_c + u_2 \times (1 - a)$ is the corrected tip resistance (MPa) (Campanella, Gillespie & Robertson, 1982), q_c is the tip resistance measured from CPT (MPa), u_2 is the measured pore pressure

behind the cone tip, $a = \frac{A_N}{A_T}$ is the net area ratio, A_N and A_T are respectively load transfer area

behind the cone tip and cross-sectional area at the base of cone tip, σ_{v0} is the vertical total stress (MPa), $\sigma'_{v0} = \sigma_{v0} - u_0$ is the vertical effective stress (MPa), u_0 is the in-situ pore water pressure (MPa) and f_s is the sleeve friction ratio (MPa).

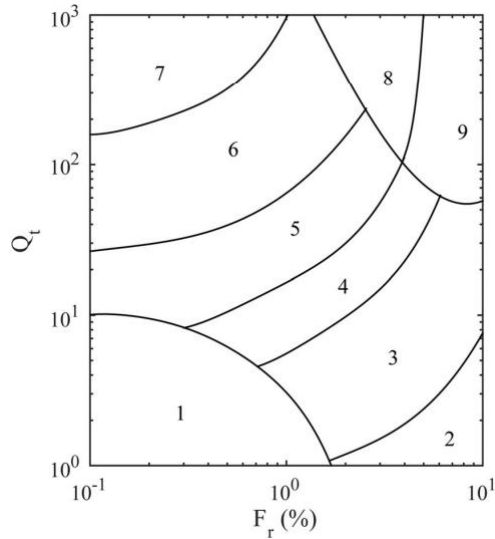


Fig. 1. Robertson's soil classification chart based on CPT with normalized friction ratio and cone resistance (1990)

Area	Soil description
1	Sensitive, fine-grained
2	Organic soils (peats)
3	Clays (clay to silty clay)
4	Silt mixtures (clayey silt to silty clay)
5	Sand mixtures (silty sand to sandy silt)
6	Sands (clean sand to silty sand)
7	Gravelly sand to sand
8	Very stiff sand to clayey sand
9	Very stiff, fine-grained

Fig. 2. Soil behaviour type description based on Robertson’s chart (1990)

In Netherlands, there is a website (<https://www.dinoloket.nl/en>) which offers open-source CPT profiles with a .GEF format and in Chapter 5, for the real case study, three CPTs are acquired from the website. Those .GEF files can be read by a CPT processing script built up by Guido de Zeeuw and it will classify the CPT data automatically based on the aforementioned chart. This script can be divided into two part: reading CPT and classifying based on Robertson’s chart. The classifying part is extracted and used individually in Chapter 4 because there are no real CPTs to be read. The exemplary processing result by using this script is shown in Fig. 3.

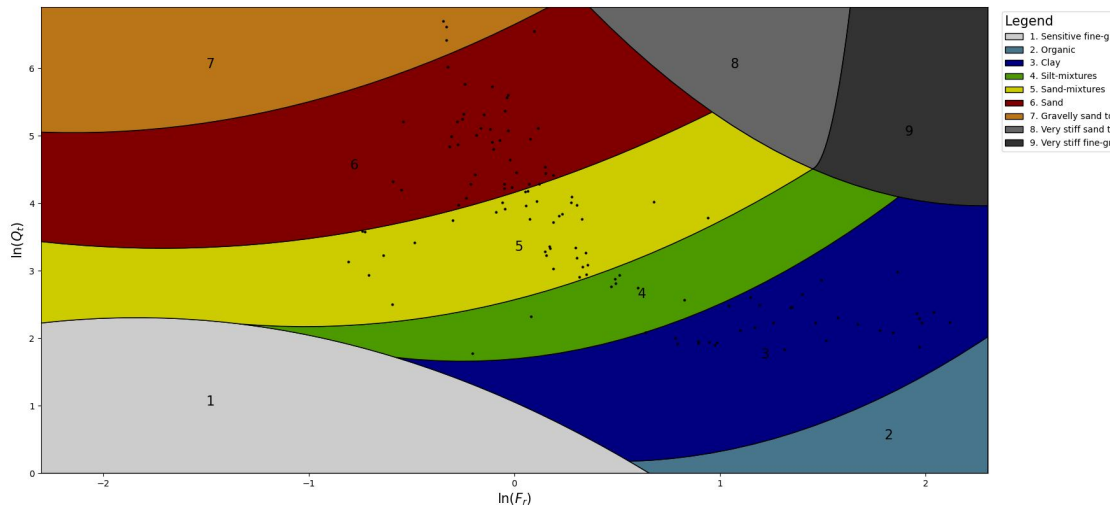


Fig. 3. An example to the result of CPT processing script

As it can be seen, the result of this script is in logarithmic scale. So actually Fig. 1 is used in the way as shown in Fig. 4.

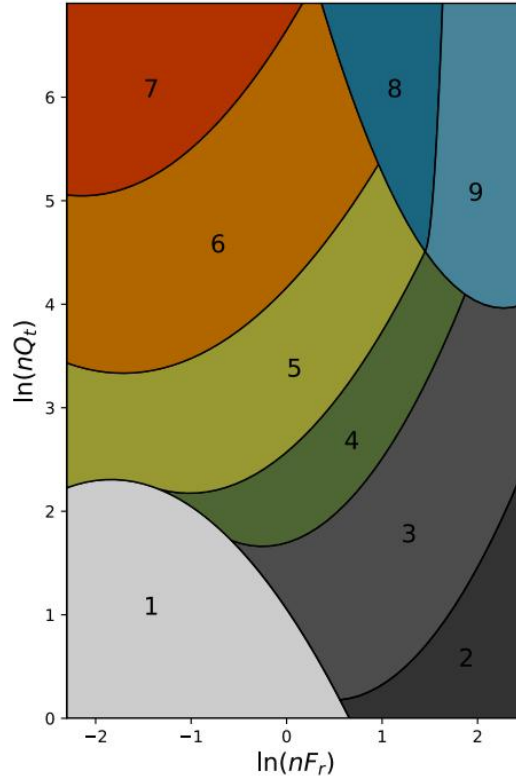


Fig. 4. Robertson's soil classification chart based on CPT with logarithmic normalized friction ratio and cone resistance (1990)

3.2 Conditional random field generator based on LAS and Kriging

3.2.1 Random field generator based on Local Average Subdivision

The random field generator used in this study is based on Local Average Subdivision (LAS) method, which was first proposed by Fenton (1990). The procedures of this method can be conceptually viewed in Fig. 5. From the stage 0 to stage 3, this is the process to subdivide the random field, which will continue until the needed maximal subdivisions. As for how to calculate the values in each cell, for example, in stage 3, the values of B1, B2 and B3 are determined by a random number generator and parent cell values. For the former one, it is built up based on the mean (μ), standard deviation (σ), scale of fluctuation (θ) as well as anisotropy of heterogeneity (ξ , the ratio between the horizontal and vertical scale of fluctuation) of the investigated material property. For the latter one, not only the cell P, but also the cells surrounding P are parent cells. Then for the value of A, upward averaging is taken, which means $(A + B1 + B2 + B3)/4 = P$. Pay attention the initial global mean (Z10) here is NOT equivalent to the mean of the system. Instead it will be determined by the scale of fluctuation and the problem domain, which won't be elaborated in this study. Additionally, if the field is anisotropic (the scale of fluctuation is different in horizontal and vertical direction), it will be squashed as it can be seen in the right part of Fig. 5. Taking $\xi = 2$ for example, the vertical direction size is reduced by a factor of 2, later the cell size will go back to the original size by taking average of the two small cells. This is the basic method used in this research.

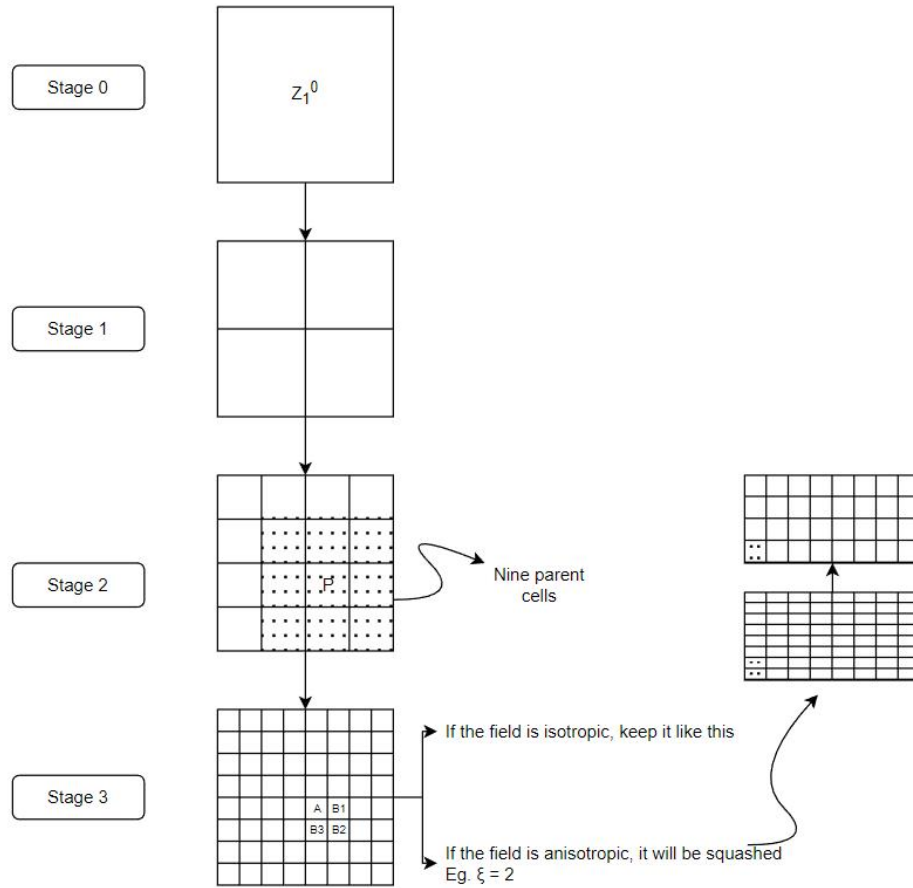


Fig. 5. Local Average Subdivision process

The LAS generator is mainly built up in Fortran by Divya Varkey and there is a pseudo code to show how to achieve step by step in Fig. 6.

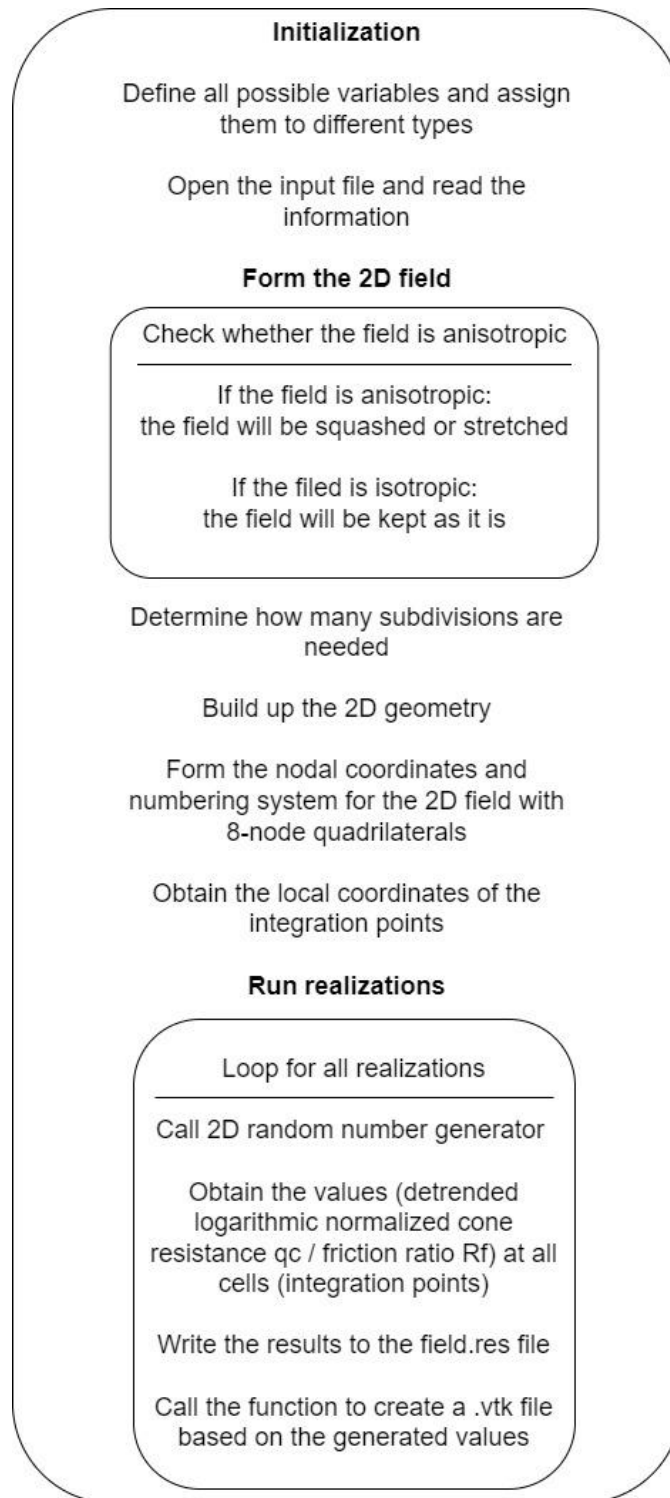


Fig. 6. Pseudo code for building random field generator based on LAS in Fortran

3.2.2 Condition random field generator based on LAS and Kriging interpolation

Furthermore, the model can be improved to be more realistic and precise by adopting conditional random field (also implemented by Divya Varkey). This can be achieved by using Kriging interpolation method. Basically this method can be explained in the following equations (Lloret-Cabot, Hicks & van den Eijnden, 2012).

$$Z^*(x_0) = \sum_{\alpha=1}^n \lambda_{\alpha} Z(x_{\alpha}) \quad (5)$$

$$\sum_{\alpha=1}^n \lambda_{\alpha} = 1 \quad (6)$$

$Z^*(x_0)$ is a material property at a location x_0 , which can be obtained from a linear combination of the known values of Z at various measured points (i.e. $Z(x_{\alpha})$). λ_{α} are n unknown weights, to be determined so as to find the best estimate for Z at x_0 .

It is worthy noticing that the Kriging interpolation cannot be directly applied to conditional random field analysis because there actually are no random variations over realizations. Instead, a superposition algorithm is adopted (Fenton & Griffiths, 2008):

$$X_c(z) = X_u(z) + X_m(z) - X_s(z) \quad (7)$$

where $z = (z_1, z_2)$ is the location along which z_1 and z_2 are sampled and unsampled; X_c is the conditional simulation; X_u is the unconditional simulation (In this study X_u is the results generated by the unconditional random filed generator mentioned in Section 3.2.1); X_m is the Kriging prediction based on measured values; X_s is the Kriging prediction based on unconditional simulation.

Similarly, there is a pseudo code in Fortran in Fig. 7. One thing deserves noticing is that when there is no real CPT data as input, the program will take realization 1 as the CPT input. It will be elaborated later in Section 4.2.2.

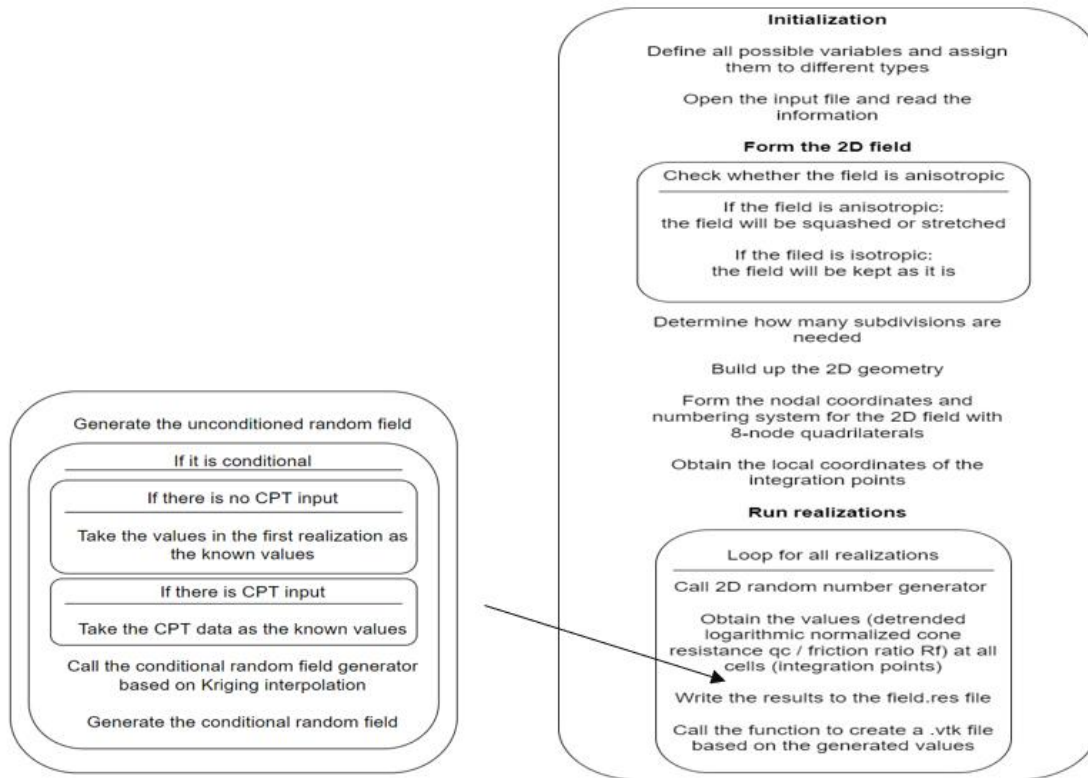


Fig. 7. Pseudo code for building conditional random field generator based on LAS and Kriging interpolation in Fortran

3.3 Input parameter identification

For the random field generator, there must be input for the mean, standard deviation and scale of fluctuation of the value to be generated. In this study, there are two proposals how to determine those input. Proposal one is to use mean and standard deviation which can cover all classifications in Robertson’s chart. This proposal departs from the idea that because of the inherent variability of the soils, any type of soil possibly exists in between two adjacent CPTs. So it is reasonable to use the mean and standard deviation, which can cover all possibilities (classifications). Specifically, the mean and standard deviation for logarithmic normalized cone resistance and friction ratio for this proposal is shown in Table 1.

Table 1. Mean and standard deviation used in the first proposal

	mean	standard deviation
$\ln(nQt)$ [MPa]	3.5	1
$\ln(nFr)$ [%]	0	0.7

Another proposal is to use the average value of measured data (tip resistance and friction ratio) over all CPT profiles as the input mean and use the average of standard deviation for each CPT

profile as the input standard deviation (Lloret-Cabot, Hicks & van den Eijnden, 2012). For scale of fluctuations, the vertical scale of fluctuation is determined by correlation function fit method, which compares the experimental correlation function plot and theoretical Markov correlation function to see which value of θ_v fits best. The horizontal scale of fluctuation is determined by the principle that the natural deposit has a ξ more than 25.

3.4 Automatic data processing

Countless data will be generated by the conditional random field generator, so a series of scripts must be made to process the data automatically and produce the meaningful results. Those scripts are mainly created in Python. Fig. 8 is the pseudo code which illustrates the main process. After running enough realizations, the results for all realizations are store in a res file. Here the results mean the generated logarithmic normalized tip resistance and friction ratio. Subsequently the aforementioned CPT classification script will be applied. So now the classifications for all realizations have been obtained, which later will be split into classifications for each realization and written in separate .vtk file. The .vtk file can be shown in Paraview to achieve the data visualization.

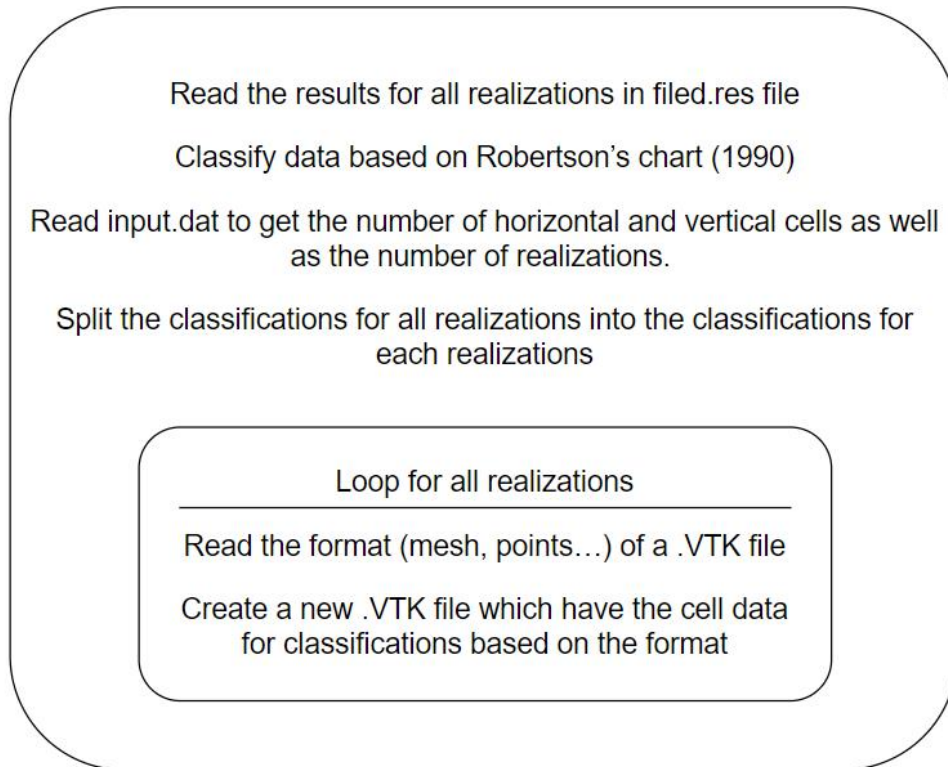


Fig. 8. Pseudo code for the main process to process generated random values

There is one remaining demand to successfully run the above script: determining how many realizations are enough. The way to figure out how many realizations are enough is to add ten more realizations to the current number of realizations and compare the change of a certain result.

If the change of such a result is less than the tolerance, the number of realizations is enough. Specifically, the result used to compare is the uncertainty of the most probable classifications and the tolerance is 0.05% (Shi & Wang, 2021b). The pseudo code is shown in Fig. 9.

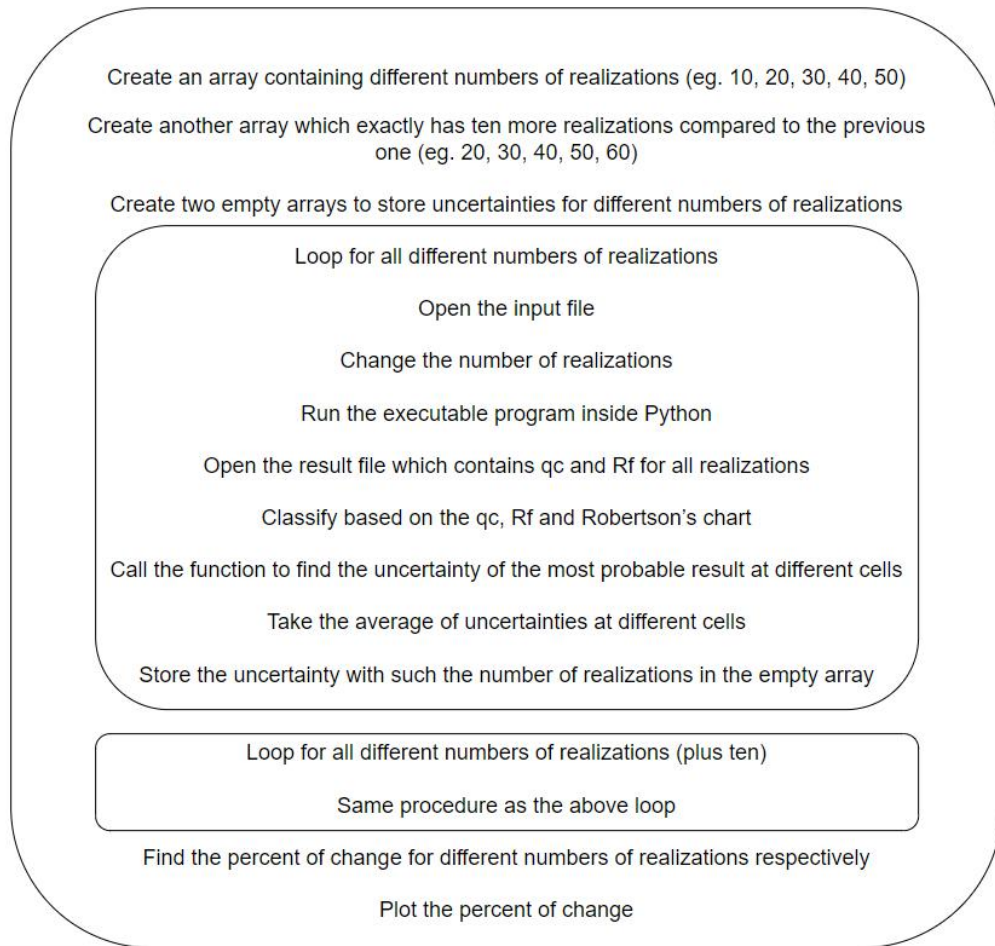


Fig. 9. Pseudo code for determination of the number of realizations

There is a subsequent demand to successfully run script shown in Fig. 9: how to find the uncertainty of the most probable result. Actually the prior demand is to determine what the most probable result is. It is not a certain realization but a comprehensive result which reflects the classification that appears most frequently over realizations at each cell. For example, for a certain cell, after 5 realizations, the classifications are respectively 3, 4, 5, 5, 5. Then type 5 is the most probable classification for this cell. The most probable classifications for all cells can be determined in the same way. Thus the most probable result can be obtained. The uncertainty of the most probable result is the average uncertainty of each cell. The uncertainty of each cell is to calculate ratio between the classifications which are different from the most probable classification and the number of realizations. Using the same example early in this paragraph, the uncertainty of the cell is 40%. This uncertainty is also known as dispersion (Shi & Wang, 2021b). The dispersion can be calculated by the following formula:

$$Dp(x) = \frac{\sum_{r=1}^{N_r} I[Z_r(x) \neq Z_{mp}(x)]}{N_r} \quad (8)$$

where $Dp(x)$ is dispersion at location x ; $Z_r(x)$ is the categorical variable of r th realization at location x ; $Z_{mp}(x)$ represents the most probable classification value at location x ; N_r denotes the total number of realizations. The pseudo codes for those two demands are shown in Fig. 10 and Fig. 11.

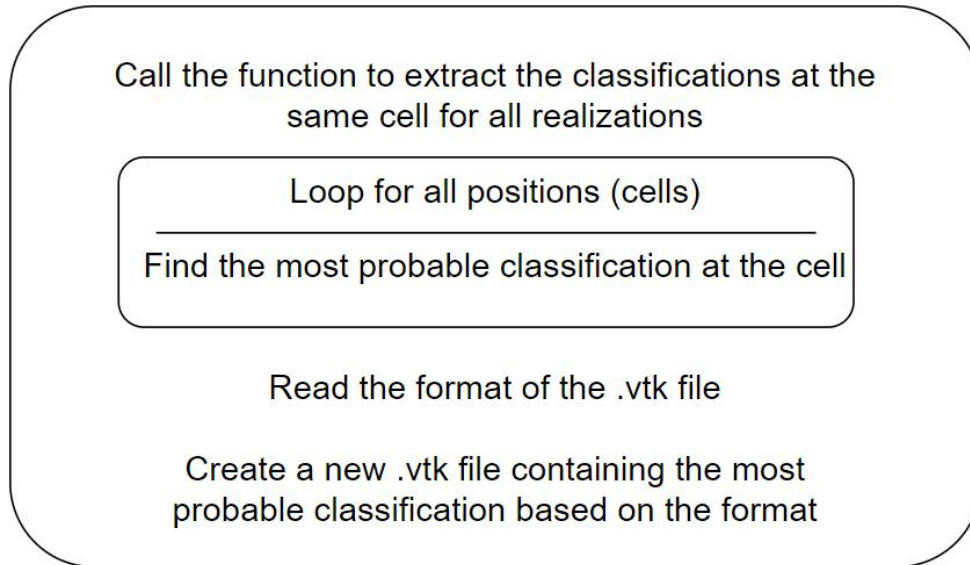


Fig. 10. Pseudo code for determination of the most probable result

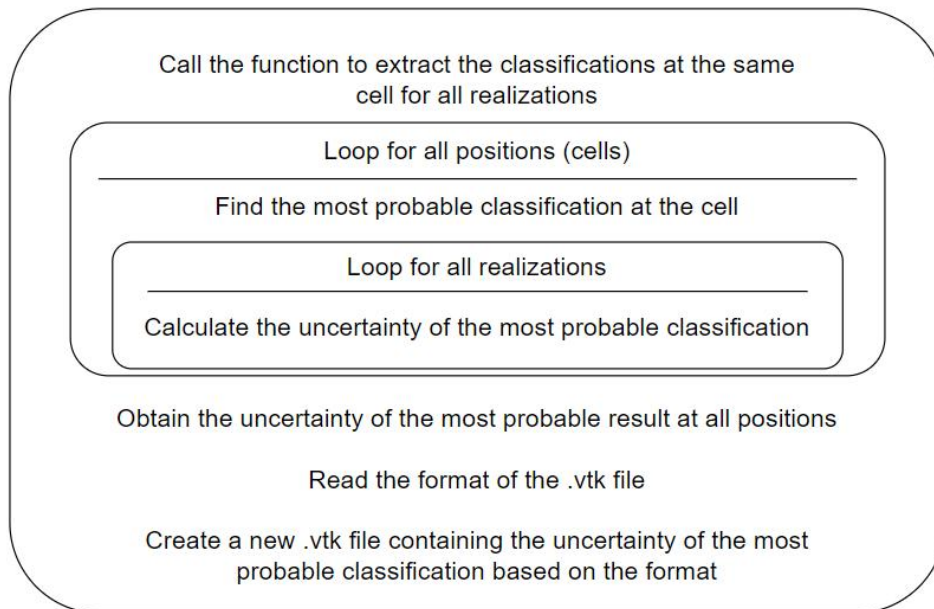


Fig. 11. Pseudo code for determination of the uncertainty of the most probable result

There is a lastly remaining demand: extracting the classification results for each cell over realizations. The pseudo is shown in Fig. 12. The code implementation for pseudo codes from Fig. 8 to Fig. 12 is shown in Appendix A to Appendix C.

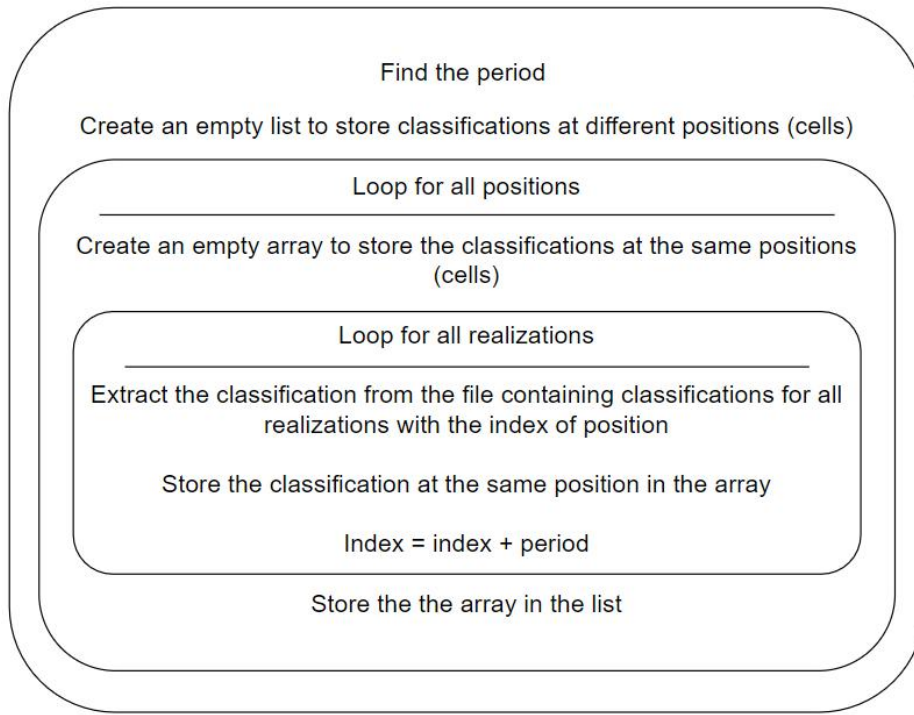


Fig. 12. Pseudo code for extraction of the classifications at the same cell over realizations

4. Illustrative example

4.1 Input determination

In this part, there is an example to show what can be obtained from the generator and accessory scripts. How to determine the input for the generator is firstly described. Fig. 13 shows the input file. The number of realizations is left to be determined after determining all the rest of input. The domain size is 20m by 10m. The mean, std are values which can cover all the classifications in the Robertson's chart, which correspond to Table 1. The vertical scale of fluctuation in this example cannot be calculated by the correlation function fit method because there are no available real CPTs. So θ_v is assumed to be a reasonable value (e.g. 1m) and the horizontal one is assumed to be 30m (for natural soil $\xi > 25$). The element size then can be calculated as $\theta_v/4 = 0.25m$ (Hicks, 2009).

Notice in this generator there is only one integration point in an element so the cell size is equal to the element size. Since there are no available CPTs, after switching to conditional random field generator, the program will automatically choosing realization 1 as the input CPT which will be used for Kriging interpolation and won't be changed in the following realizations. Notice not all columns are be taken as the input CPT but the columns where the user set to have conducted CPTs. In this example, as can be seen in raw 9 in Fig. 13, there are three columns to have CPTs, respectively corresponding to column 0, column 40 and column 79 (the numbering starts from 0). The unconditional results are also generated from the program, which can be used for the comparison between conditional and unconditional scenarios.

Now moving backing towards the number of realizations, it is determined by the script shown in Appendix B. Other inputs remain the same for different numbers of realizations. It can be seen in Fig. 14, when the number of realizations is equal to 100, the percent of change is around 0.01%, which is smaller than the tolerance (0.05%). So it is logical to run for 100 realizations.

```
100
80 40
0.25 0.25
0 0.7 3.5 1
-2602051
1.0 30 .false.
.true.
.false.
0 3 39

# no. of realisations
# no. of elements along x and z
# size of elements along x and z
# mean of field 1, sd. of field 1, mean of field 2, sd. of field 2
# seed
# theta in vertical, anisotropy in horizontal, lognormal
# conditioned
# CPT data in a file
# position of 1st CPT, no. of CPTs, no. of elements between adjacent CPTs
```

Fig. 13. Input for the illustrative example

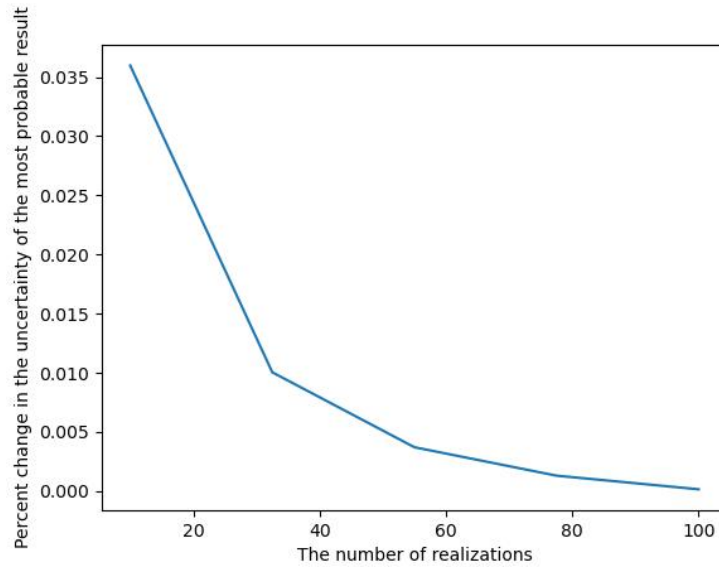


Fig. 14. Percent change in the uncertainty of the most probable result over realizations

4.2 Results and analysis

Subsequently, the generated data is processed by the aforementioned Python scripts from Appendix A to Appendix C and Fig. 15 to Fig. 20 show the final results.

4.2.1 Most probable result for classifications and its uncertainty

The most probable result is shown in Fig. 15 and it can be seen that the main soil type is 5. This is because the middle part of Robertson's chart is chosen as the mean, so type5, which locates in the middle of the chart, appears most frequently. The uncertainty is shown in Fig. 16 and the average uncertainty is 17.2%. It can be seen that the uncertainty decreases as the cell approaches to any side of the adjacent CPTs. In other words, the uncertainty is the highest in the middle part of two adjacent CPTs while the uncertainty is the lowest (actually 0%) in the conducted CPT positions. This phenomenon is in alignment with the reality.

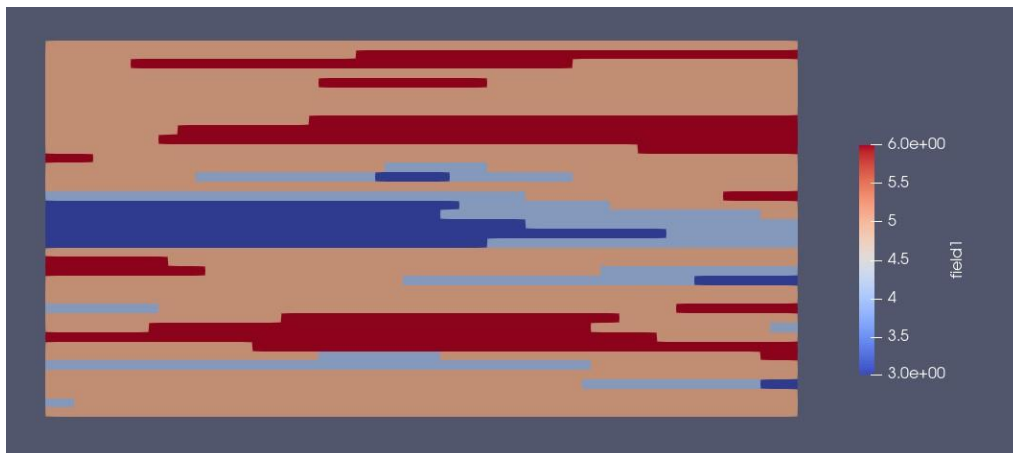


Fig. 15. The most probable result of classifications in the illustrative example

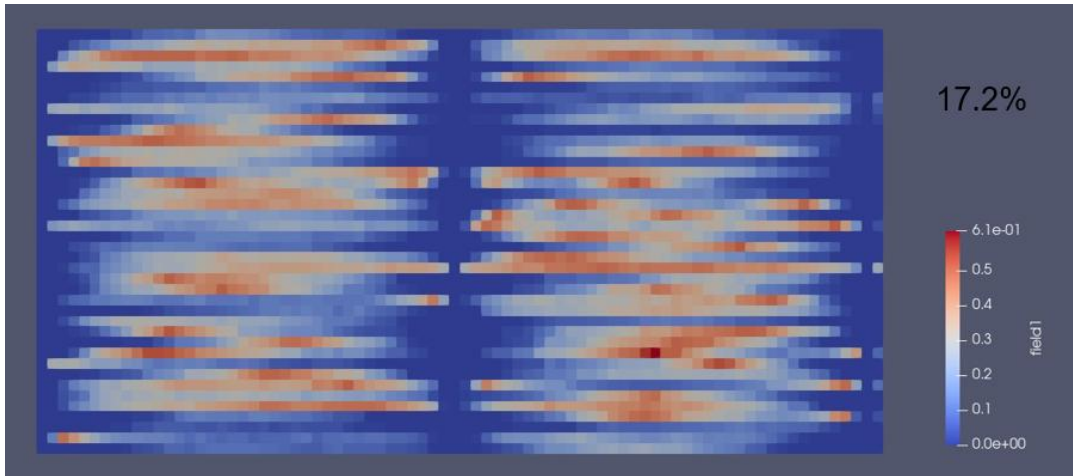


Fig. 16. The uncertainty of the most probable result of classifications in the illustrative example with an average uncertainty of 17.2%

4.2.2 Comparison between conditional and unconditional random field generator

The first comparison is to show what the difference between conditional and unconditional random field generator is. For conditional scenario, as mentioned earlier, in all realizations the classifications at conducted CPT positions don't change, while for unconditional scenario, there is no such a constrain. This phenomenon can be seen in Fig. 17 and Fig. 18. For simplicity, only column 0 is compared. In addition, no matter it is conditional or unconditional scenario, the 1st realization is always the same as shown in Fig. 19.

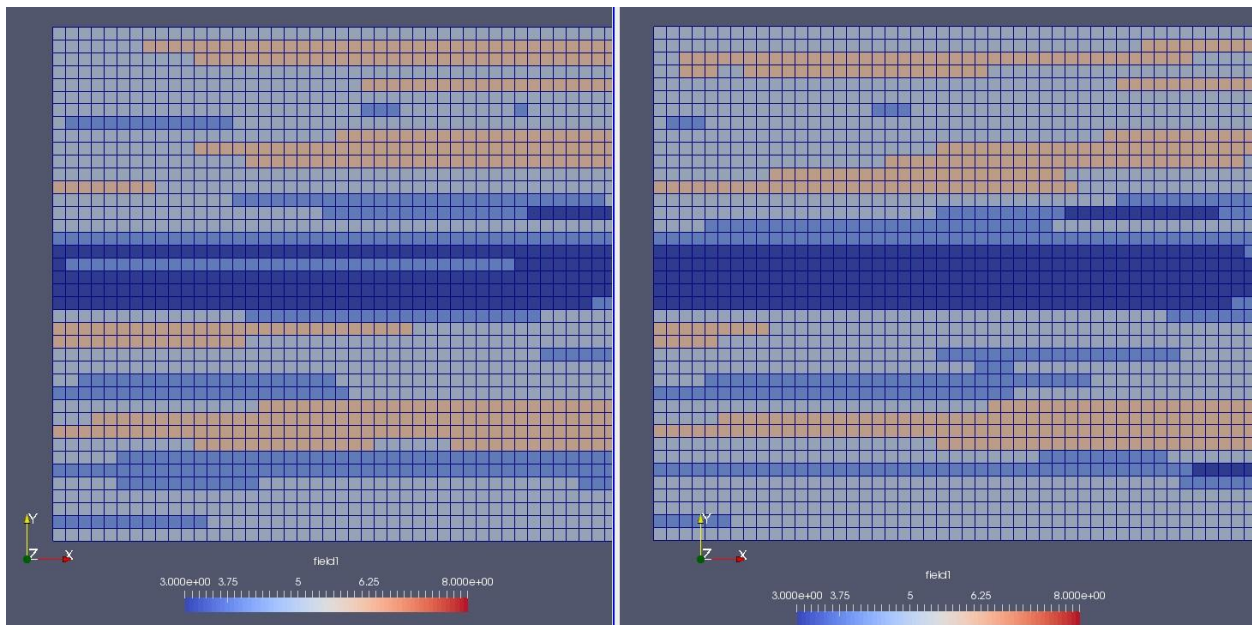


Fig. 17. The classifications in the first and second realization in conditional random field, comparing the first column on the left side

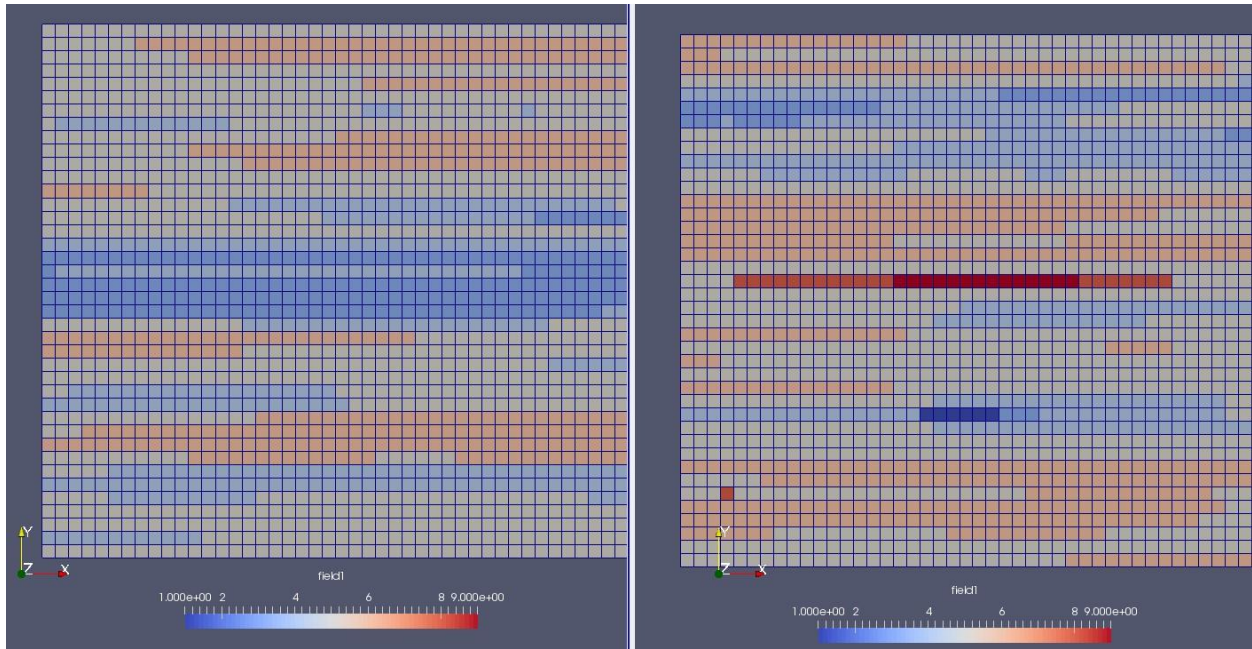


Fig. 18. The classifications in the first and second realization in unconditional random field, comparing the first column on the left side

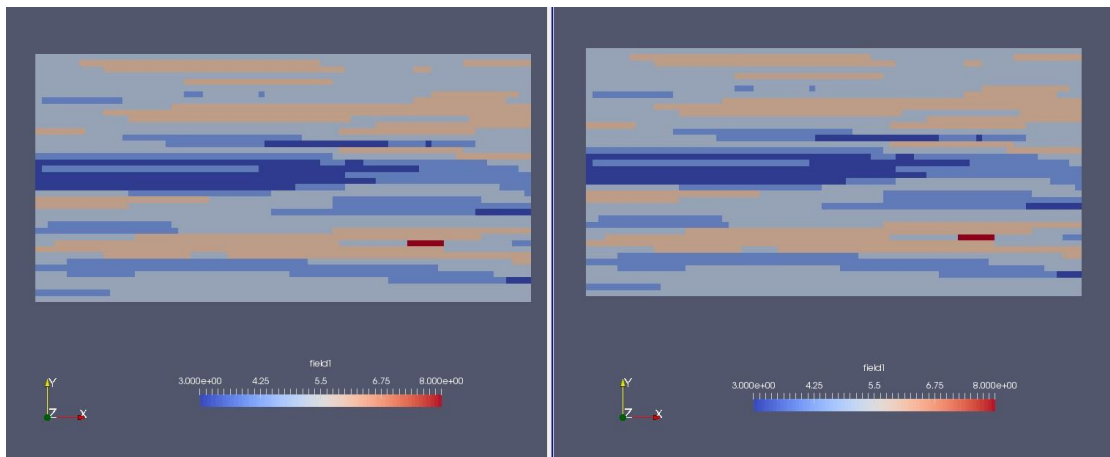


Fig. 19. The classifications of the first realization in conditional random field (left) and unconditional random field (right)

Moreover, the average uncertainty of the conditional and unconditional random field generator can be compared. It is shown in Fig. 20. It is evident that the average uncertainty is higher in unconditional scenario, which is logical because for the conditional generator, based on Kriging interpolation, there is more information extracted from the real CPTs or there are more constrains from the real CPTs for the random field. So definitely the uncertainty is reduced in conditional random field.

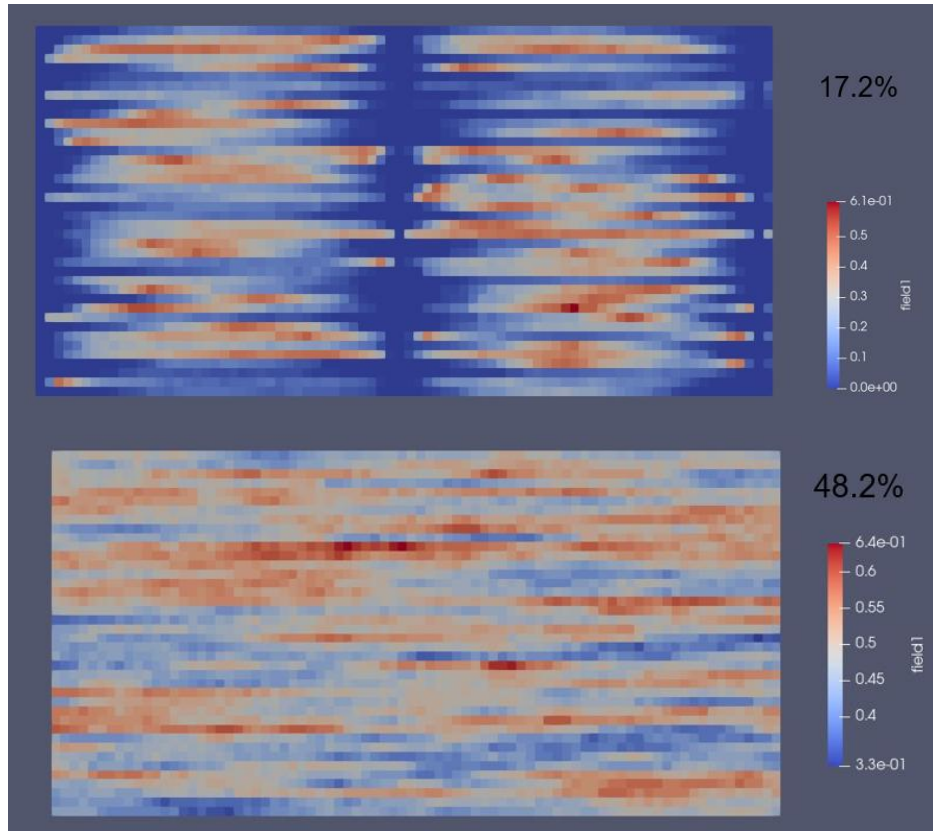


Fig. 20. The average uncertainty comparison between the conditional random field (17.2%, upper) and the unconditional random field (48.2%, lower)

4.2.3 Convergence in the unconditional random field

Since in the unconditional random field, the generation of random values doesn't take Kriging interpolation into consideration, there is one speculation that with the increase of realizations, the most probable classifications for each cell will converge to a certain type. Additionally, because the generation conforms with Gaussian distribution shown in Fig. 21, the convergence type is speculated to be type 5.

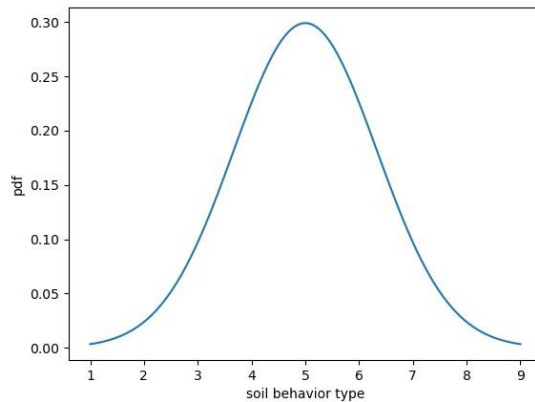


Fig. 21. The normal distribution of soil behaviour type

The method is similar to the method to determine how many realizations are enough. Specifically, the current most probable result and the most probable result with ten more realizations are compared but this time the focus is on the classifications instead of the average uncertainty. The result is plotted in Fig. 22. The difference refers to the difference between two most probable results of classifications. For each cell, if the classification is different when the number of realizations is n and when the number of realizations is $n+10$, the counter will be added by 1. After looping for all cells, counter will be divided by the total number of cells and that is the difference. It can be found that as the increase of realizations, the difference tend to be 0. So it proves the speculation that in unconditional random field, the classification for each cell tends to converge when there are enough realizations.

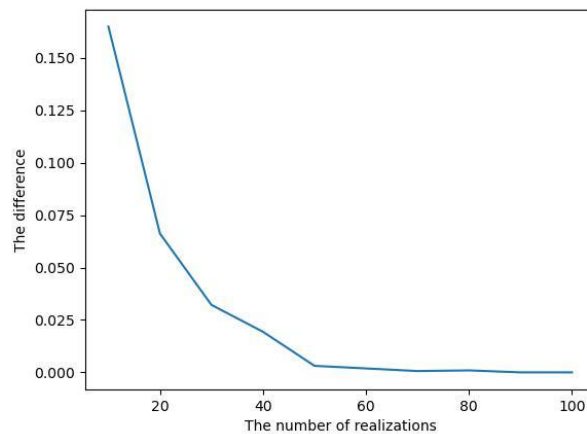


Fig. 22. The difference between the most probable result of classifications of n realizations and $n+10$ realizations in unconditional random field

Additionally, the most probable result for 100 and 110 realizations can be viewed in Paraview to have a more direct comparison. They are shown respectively in Fig. 23 and Fig. 24. It can be also seen that the convergence type is type 5, which conforms with the second speculation.



Fig. 23. The most probable result ($r = 100$)



Fig. 24. The most probable result ($r = 110$)

Finally, with the increase of the number of realizations, actually the average uncertainty has no big changes. It is also logical because the mean can only contain around 50% reliability. It's shown in Fig. 25.

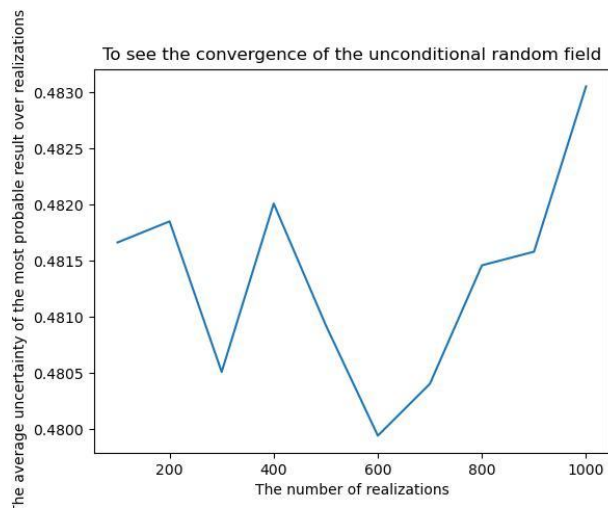


Fig. 25. The average uncertainty in the unconditional random field over realizations

Whereas in the conditional field, because the existence of Kriging interpolation, the classifications in each cell cannot converge no matter how many realizations are. The difference exists permanently, which is shown in Fig. 26.

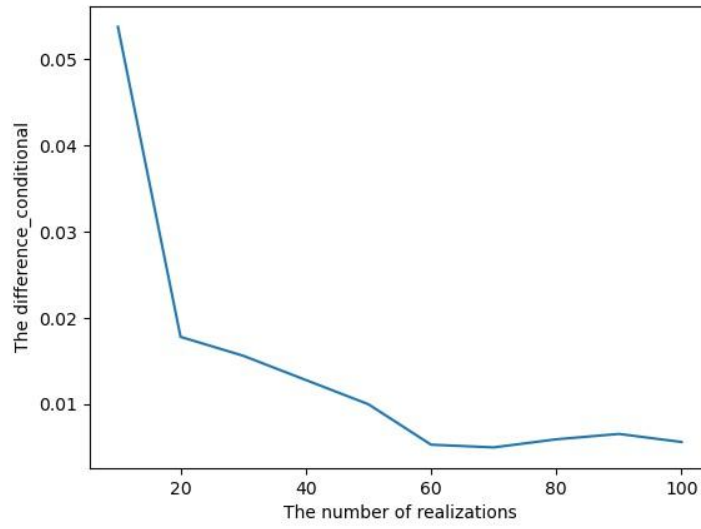


Fig. 26. The difference between the most probable result of classifications of n realizations and $n+10$ realizations in conditional random field

5. Case Study

5.1 Background

In this part, the proposed conditional random field generator is applied to a real case, which aims to achieve probabilistic soil classifications using three conducted CPTs. Those three CPTs are obtained from <https://www.dinoloket.nl/en>, respectively named as CPT000000161781, CPT000000161782 and CPT000000161785. Their relative positions are shown in Fig. 27. For simplicity, their names are changed to CPT1, CPT2 and CPT5. All of them are projected to x axis and based on their coordinates, it can be calculated that the spacings are 22 m and 25 m. So in the random field, CPT1 can be approximately regarded as exactly in the middle of CPT2 and CPT5. What those three CPTs look like in the random field is shown in Fig. 28.

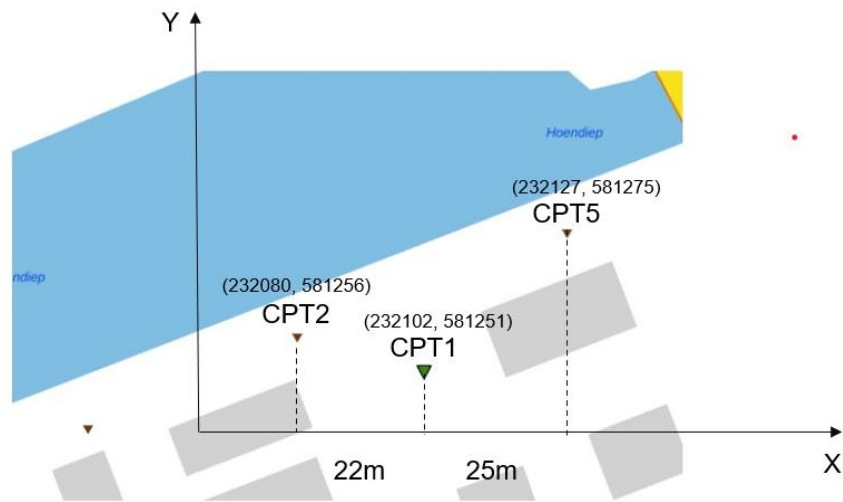


Fig. 27. The real locations of the three CPTs used in case study

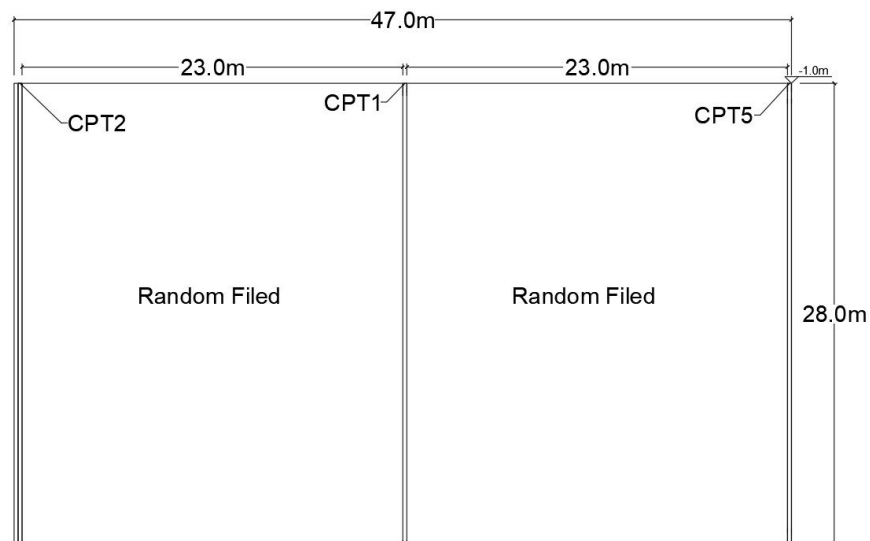


Fig. 28. The schematic diagram for the locations of the three CPTs in the random field

It's worthy noticing that because there are some differences of those CPTs in terms of the initial depth and CPT length, some data has to be deleted in order to make those three profiles uniform. After some adjustments, all CPTs start from one meter below the ground and have a depth of 28 meters. The horizontal size is 47 meters. In all, it is a 47m by 28m domain locating at one meter below the ground.

5.2 Input data

The input mean and standard deviation for this case adopt the second proposal in Section 3.3. The mean is the average values for all CPT profiles. The standard deviation is the average of the standard deviation for each CPT. Those two parameters for both cone resistance and friction ratio are calculated by Python script, which can be seen in Appendix D1. The results are shown in Table 2.

Table 2. Mean and standard deviation calculated from the three CPTs (the second proposal)

	mean	standard deviation
$\ln(nQt)$ [MPa]	3.81	1
$\ln(nFr)$ [%]	0.36	0.76

Additionally, as for the vertical scale of fluctuation, it is calculated by trying to find value which fits the Markov correlation function to the experimental correlation function. Those two functions are shown in Eq. (9) and Eq. (10) respectively:

$$\rho(\Delta z) = \exp\left(-2 \frac{\Delta z}{\theta}\right) \quad (9)$$

$$\hat{\rho}(\Delta z) = \frac{1}{n_{\Delta z}} \sum_{i=1}^{n_{\Delta z}} U(z_i)U(z_i + \Delta z) \quad (10)$$

where $U(z_i)$ and $U(z_i + \Delta z)$ are a pair of detrended random field data points at relative distance Δz , $n_{\Delta z}$ is the number of pairs available in the data at a distance Δz and θ is the vertical scale of fluctuation.

How to implement the calculation of vertical scale of fluctuation can be seen in Appendix D2. Fig. 29 and Fig. 30 show the conceptual process. For the horizontal scale of fluctuation, a reasonable anisotropy of heterogeneity is assumed to calculate $\theta_h = \theta_v \times \xi$.

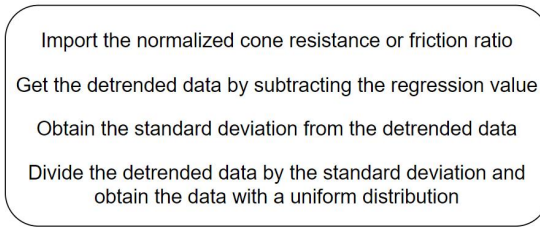


Fig. 29. Pseudo code for calculating the normalized cone resistance or friction ratio with a uniform distribution

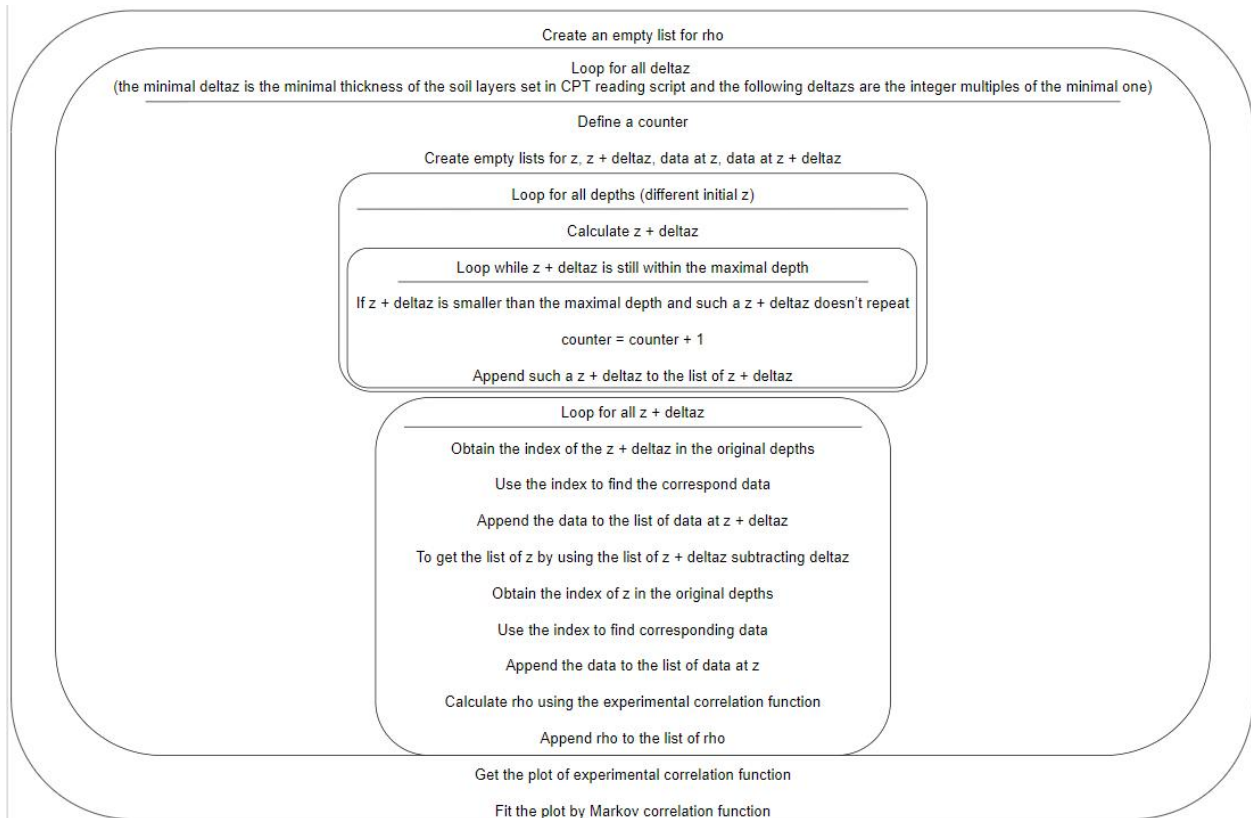


Fig. 30. Pseudo code for calculating the vertical scale of fluctuation of normalized cone resistance and friction ratio

The results of those correlation functions are shown in Fig. 31 and Fig. 32. There is a phenomenon that the latter part of those two experimental correlation function curves reach some negative values. This is because in the real CPT profile there are many variations. Thus when the relative distance is large, two points in a pair are likely to locate separately in weak zone and strong zone. Moreover, it is also caused by relatively little data and short CPT profiles. Still it can be approximately estimated that when $\theta_v = 2$ m, Markov correlation function fits best for normalized friction ratio and when $\theta_v = 3$ m, Markov correlation function fits best for normalized cone resistance. Eventually, the vertical scale of fluctuation used in the conditional random field generator is the average of these two values, 2.5m. Additionally, ξ is set to be 30, so the horizontal scale of fluctuation is 75m.

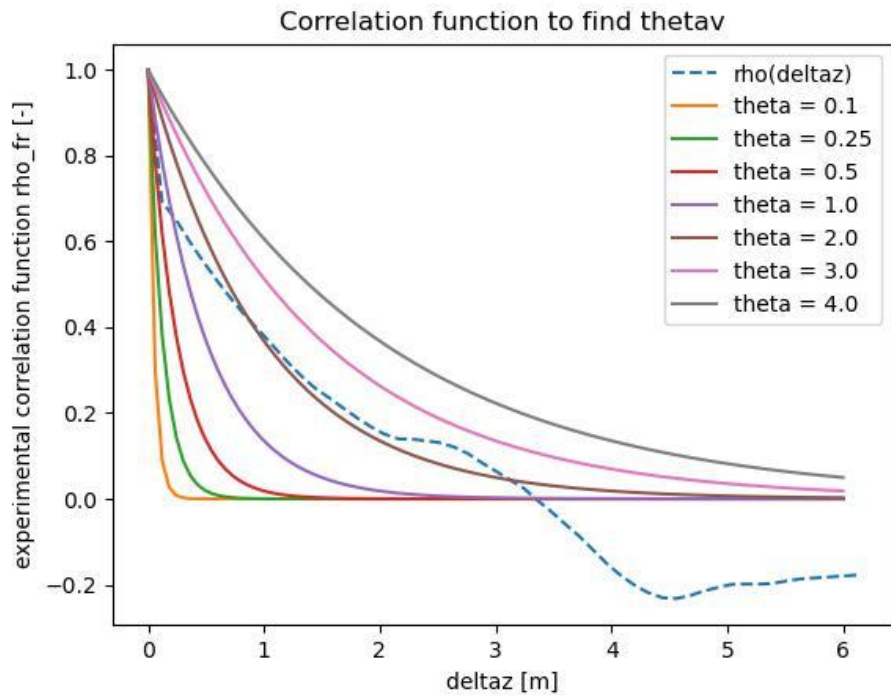


Fig. 31. The correlation function fit for normalized friction ratio

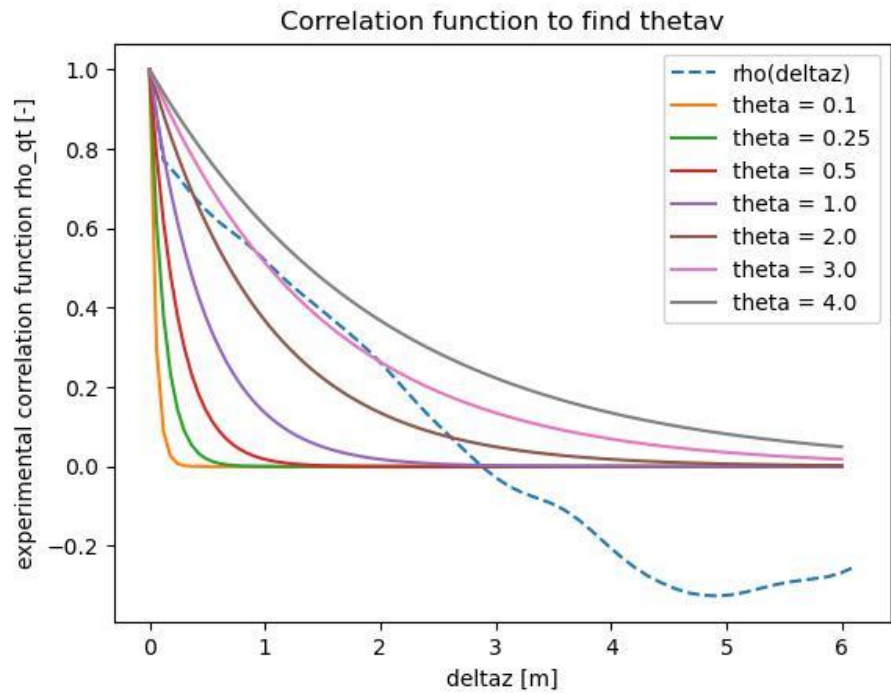


Fig. 32. The correlation function fit for normalized cone resistance

Finally, the cell size is determined by principle that the maximal cell size is no bigger than a quarter of minimal scale of fluctuation, so the cell size is chosen to be 0.5m. All the input is shown in Fig. 33.

```

100
94 56
0.5 0.5
0.36 0.76 3.81 1
-2602051
2.5 75 .false.
.true.
.true.
1 3 46

# no. of realisations
# no. of elements along x and z
# size of elements along x and z
# mean of field 1, sd. of field 1, mean of field 2, sd. of field 2
# seed
# theta in vertical, anisotropy in horizontal, lognormal
# conditioned
# CPT data in a file
# position of 1st CPT, no. of CPTs, no. of elements between adjacent CPTs

```

Fig. 33. The input for the case study

5.3 Results and analysis

Similarly, the generated data is processed by the aforementioned Python scripts from Appendix A to Appendix C and Fig. 34 to Fig. 36 show the final results.

5.3.1 Most probable result for classifications and its uncertainty

Fig. 34 illustrates the most probable result for classifications in this case study and it can be seen that type 5 is no longer predominant. This is because with the participation of Kriging interpolation and the real CPTs, the distribution for each cell doesn't conform with Gaussian distribution but is subject to the conducted CPT data. Fig. 35 shows the uncertainty of the most probable result and the average uncertainty is 4.58%. The phenomenon that, the uncertainty is the highest in the middle part of two adjacent CPTs while the uncertainty is the lowest (actually 0%) in the conducted CPT positions, can be also seen in Fig. 35.

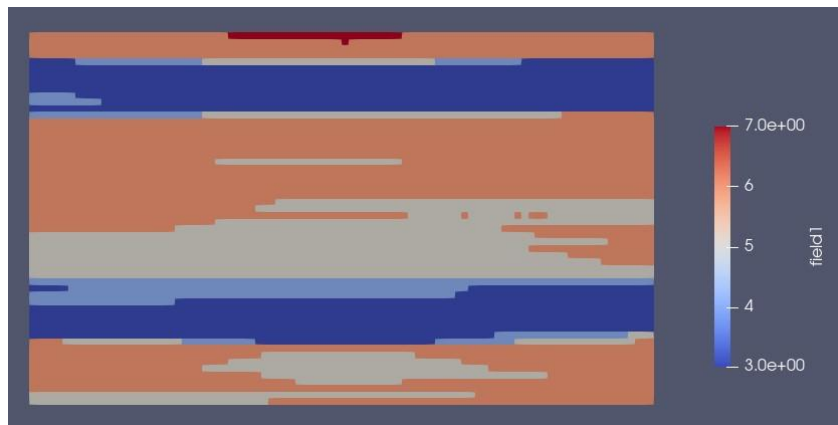


Fig. 34. The most probable result of classifications in the case study

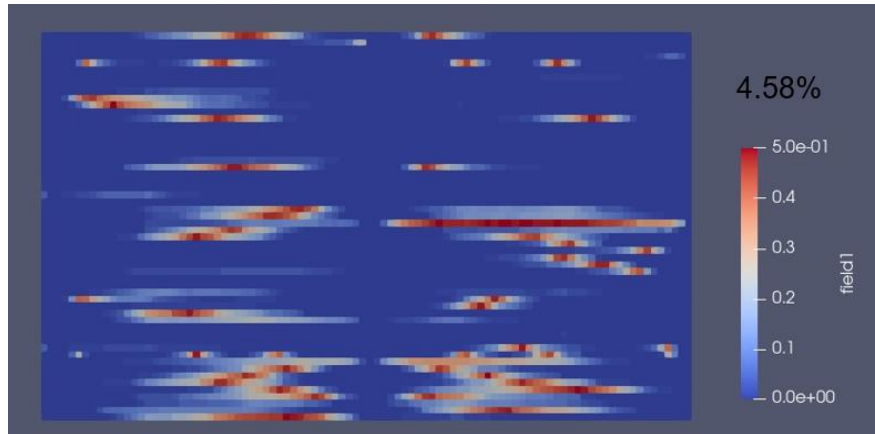


Fig. 35. The uncertainty of the most probable result of classifications in the case study, with an average uncertainty of 4.58%

5.3.2 Comparison between conditional and unconditional random field generator

It has been shown that the column where to set CPT doesn't change over realizations in the conditional random field in Chapter 4, so it's not repeated here. Only the average uncertainty is compared between conditional and unconditional random. Fig. 36 also illustrates that the uncertainty of unconditional scenario is higher than conditional scenario.

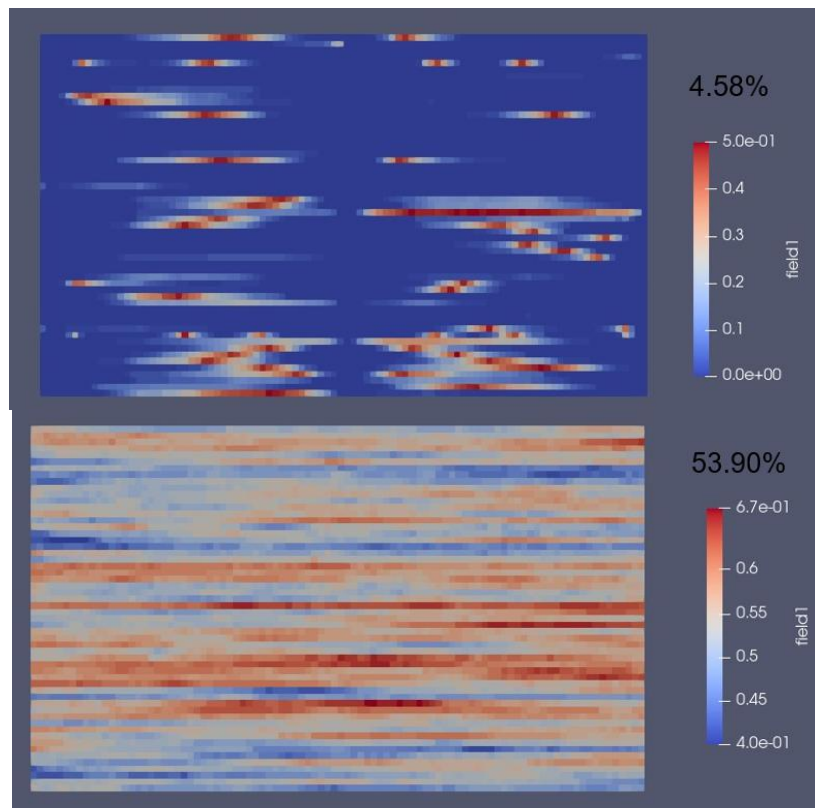


Fig. 36. The average uncertainty comparison between the conditional random field (4.58%, upper) and the unconditional random field (53.9%, lower) in the case study

5.4 Influence of one less CPT

Further study can be done within adjacent CPTs. Specifically, the central CPT (CPT1) is removed from input and other input keep the same. A few analyses are done subsequently to investigate in the influence in terms of: a) the uncertainty change after removing CPT1; b) the distribution of random values in the central column; c) the classifications of the simulated central column. The script to implement analysis b and c is shown in Appendix E.

a) The uncertainty change after removing CPT1

The most probable result of classifications and its uncertainty can be obtained by using the similar code as Appendix C. It can be observed in Fig. 38 that with only two known CPTs, the uncertainty of the classifications is 7.58% which is higher than the uncertainty of three known CPT case 4.58% shown in Fig. 35.

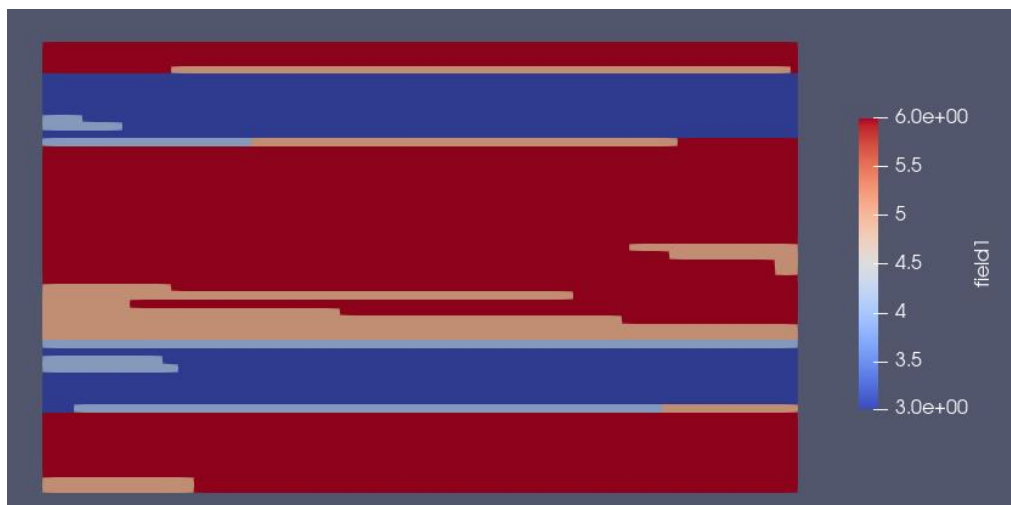


Fig. 37. The most probable result of classifications with CPT2 and CPT5

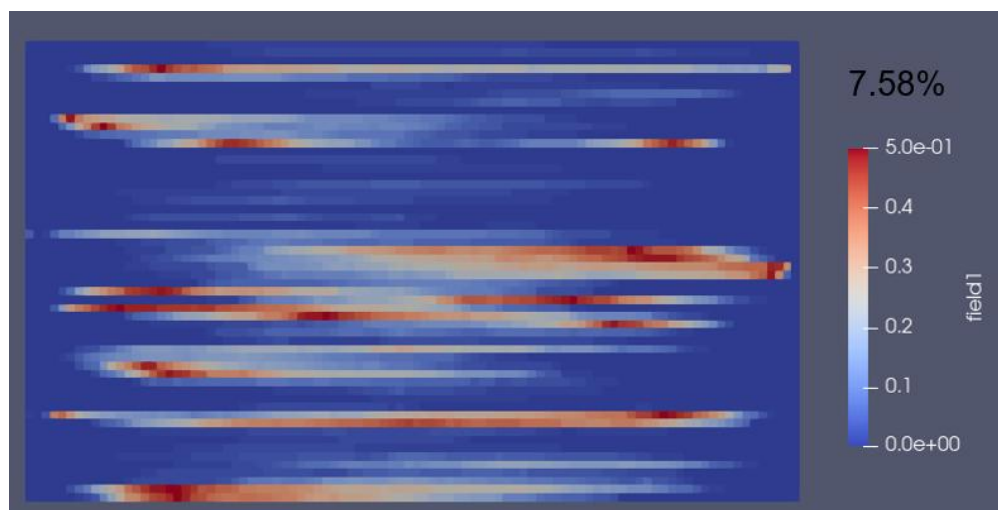


Fig. 38. The uncertainty of the most probable result of classifications with CPT2 and CPT5, with an average uncertainty of 7.58%

b) The distribution of random values in the central column

After running the conditional random field generator with 2 CPTs, the random values in the central column can be extracted over realizations. Based on those values, two post processes are taken. Both of these processes are applied to normalized friction ratio and cone resistance respectively. The first is to find the minimal and maximal value for each cell in the column over realizations. After doing this for all cells, the minimal and maximal boundary of CPT profiles can be obtained, which can be seen in Fig. 39 and Fig. 41. It's observed that the conducted CPT1 is within those two boundaries. The second process is to calculate the point statistics (mean and standard deviation) for each cell. Subsequently the representative point statistics can be calculated by taking the average of point statistics for each cell. It's worthy noticing that indeed the point statistics can vary a lot among different cells, but the coefficient of variance (COV, standard deviation / mean) doesn't vary a lot. So still it's meaningful to take such an average. Moreover, because the generation of the random values is subject to normal distribution, the probability density function can be drawn based on the point statistics and normal distribution, which is shown in Fig. 40 and Fig. 42.

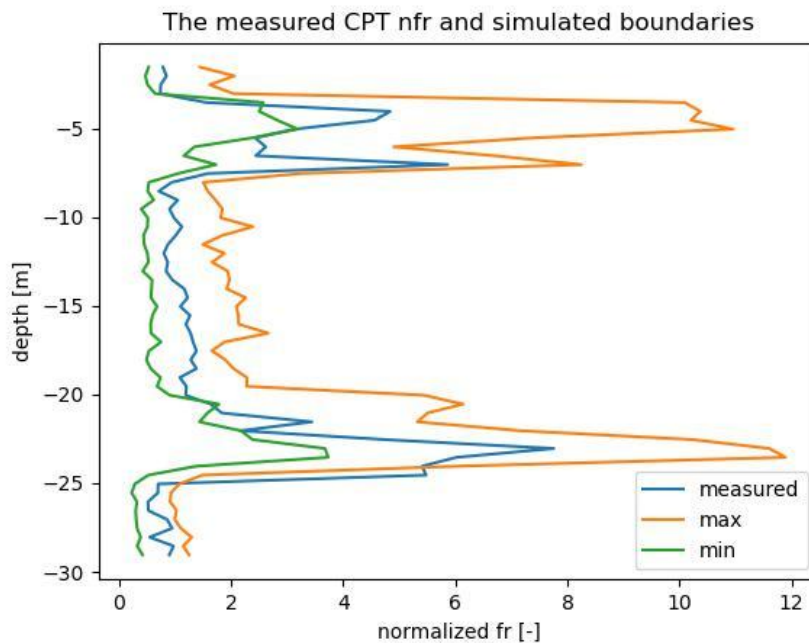


Fig. 39. The simulated boundaries of normalized friction ratio

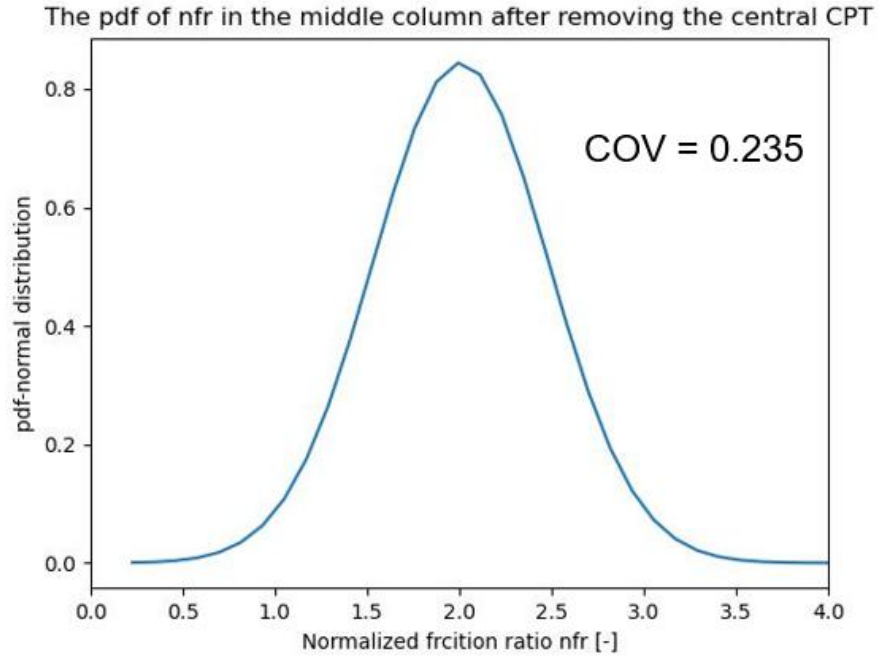


Fig. 40. The pdf of normalized friction ratio in the middle column

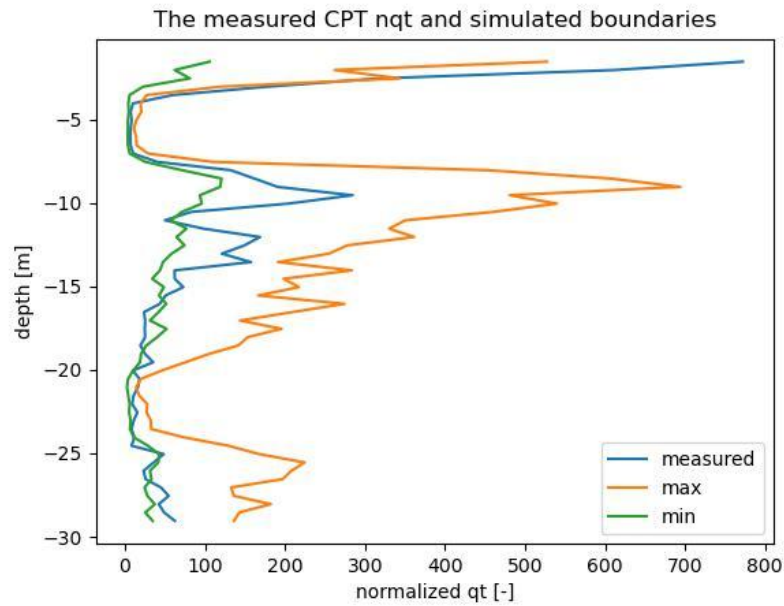


Fig. 41. The simulated boundaries of normalized cone resistance

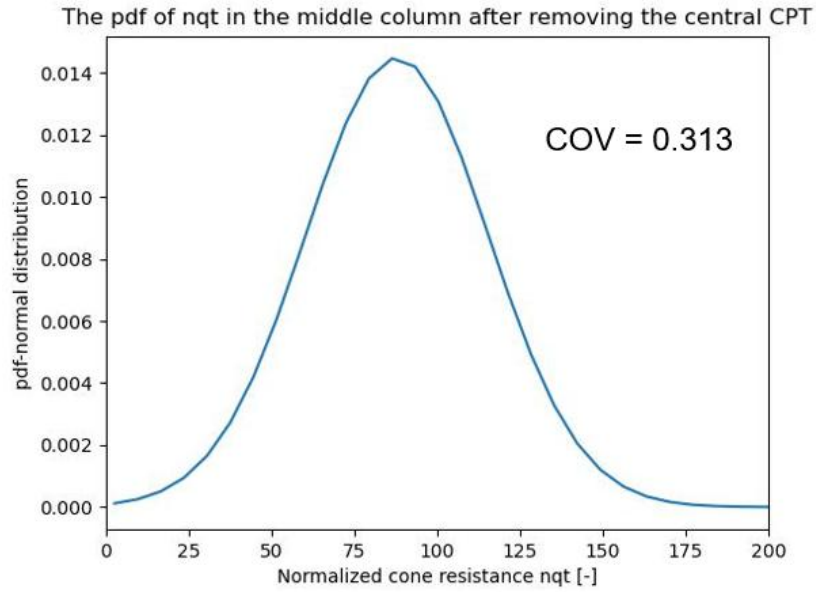


Fig. 42. The pdf of normalized cone resistance in the middle column

c) The classifications of the simulated central column

The random values generated with two CPTs input can be also applied to do classifications and the middle column is extracted to compare with CPT1 classifications. Fig. 43 illustrated the difference is 41.07%.

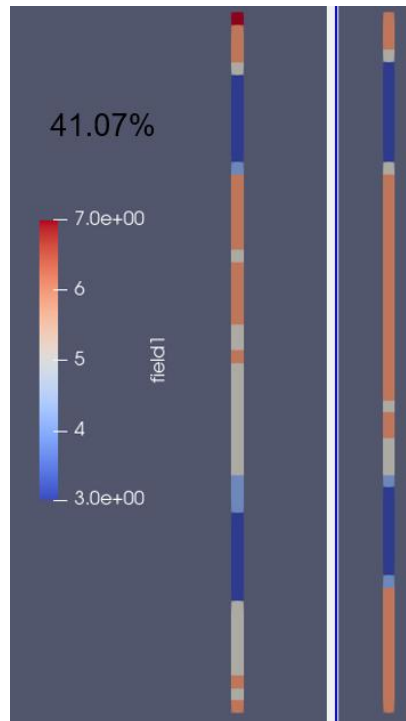


Fig. 43. The comparison between the most probable classifications in the middle column and CPT1

6. Limitation and optimization

6.1 Uncertainty in soil classification model

The proposed method to achieve probabilistic classification doesn't consider the uncertainty in classification model. Actually when using the CPT processing script to generate CPT profiles, it is in a deterministic way, which may ignore the uncertainty in CPT-based soil classification using Robertson's chart. Actually this uncertainty can be explicitly modeled in Bayesian approaches (Wang, Huang & Cao, 2013). Although this investigation is out of the scope of this study, there is an alternative and simpler way to include the consideration of uncertainty in soil classification model proposed by Hu & Wang (2020). How to calculate soil behavior type index and how to use SBT index I_c to achieve soil classifications were proposed by Robertson & Wride (1998).

The function is defined as:

$$I_c = \sqrt{(3.47 - \log Q_t)^2 + (\log F_r + 1.22)^2} \quad (11)$$

where Q_t and F_r are normalized cone resistance and friction ratio. Soil classifications based on SBT index I_c is shown in Table 3.

Table 3. Soil classifications based on SBT index, I_c (Robertson & Wride, 1998)

Range of SBT index I_c	SBT ID	SBT description
$I_c < 1.31$	7	Gravelly sand to dense sand
$1.31 < I_c < 2.05$	6	Sands: clean sand to silty sand Sand mixtures: silty sand to
$2.05 < I_c < 2.60$	5	sandy silt Silt mixtures: clayey silt to silty
$2.60 < I_c < 2.95$	4	clay
$2.95 < I_c < 3.60$	3	Clays: silty clay to clay
$I_c > 3.60$	2	Organic soil: peats

It can be seen that there are some boundaries for I_c respectively: 1.31, 2.05, 2.60, 2.95, 3.60. Means and standard deviations can be given to them in order to carry on the stochastic approach, which is shown in Table 4.

Table 4. Probabilistic boundaries of SBT index, I_c (Hu & Wang, 2020)

Statistics	B1	B2	B3	B4	B5
Mean	1.31	2.05	2.6	2.95	3.6
Standard deviation	0.1	0.1	0.05	0.05	0.1
Range	[1.01, 1.61]	[1.75, 2.35]	[2.45, 2.75]	[2.8, 3.1]	[3.3, 3.9]

As for how to use it specifically, for example, there are 100 realizations for normalized cone resistance and friction ratio, which later are applied to Eq. (11) to obtain I_c , from the proposed conditional random field generator based on LAS. At the mean time, there can be 100 sets of boundary values for I_c from a simple probabilistic model based on Table 4. Those 100 realizations are classified by corresponding 100 sets of boundaries. As a result, there are 100 probabilistic soil geographies which simultaneously incorporate uncertainties in the soil classification model as well as the uncertainties in the classification result.

6.2 Combination with boundary based model

The generator used in this study is basically category-based but actually it is more precise and realistic to carry on boundary analysis before the conditional random field category analysis. So the proposed method can be optimized by adding a boundary-based model in the random field. This can be achieved by a heuristic model (Xiao, Zhang, Li, & Li, 2017). First, the boundaries at conducted CPT positions can be determined, which will be used as known values for Kriging interpolation and unconditional random field simulation for boundaries in between adjacent CPTs. Notice Kriging interpolation cannot be solely applied because it actually has no random variations. Subsequently those simulated boundaries as well as the real boundaries measured by CPTs are used as constrains for the category based random field analysis. This is to say, with this method, the constrains of the conditional LAS random field generator come from both the boundaries and the conducted 1D CPT data.

There is another method according to the claim that the locations of high uncertainty are generally consistent with the underlying true soil layer boundaries (Hu & Wang, 2020). So a conceptual process is proposed in this study which is shown in Fig. 44.

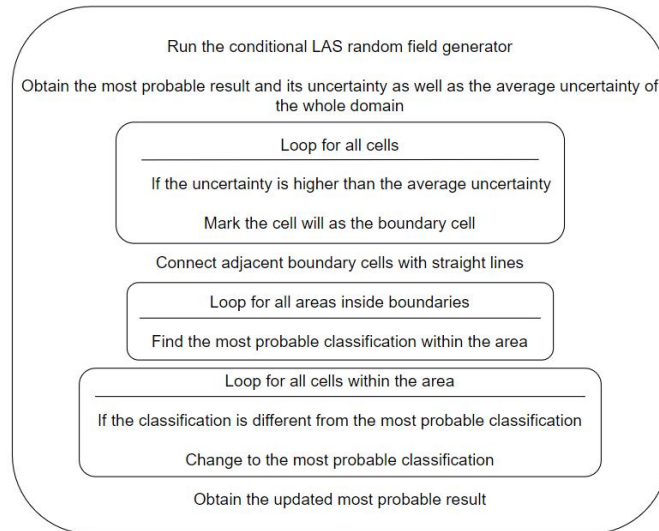


Fig. 44. Pseudo code for adding boundary based model

Notice when connecting boundary cells, it may be assisted manually. The most probable result is only one image so it is feasible and in this way prior knowledge and profession knowledge can be utilized.

7. Conclusion

A random field generator based on Local Average Subdivision (LAS) is proposed in this study which aims to achieve probabilistic soil classifications and consider the uncertainty of the geological cross section. Moreover, it has been improved to a conditional random field generator by using Kriging interpolation which exerts more constraints to the random field. The unconditional and conditional generator are tested by an illustrative example and the conditional generator is applied to a case study with three real conducted CPTs. There are a few conclusions can be drawn:

- a) It can be evidently seen that the uncertainty of the most probable result of classifications generated by the conditional random field generator (17.2%) is lower than that of the unconditional random field generator (48.2%). The uncertainty is truly reduced by improving the generator and the generation of the classifications are more realistic and meaningful.
- b) With enough realizations, the classifications in the unconditional random field converge. In the most probable result, because Gaussian distribution is the only factor considered in the unconditional generation, all classifications become type 5 which is the mean used in the unconditional random field. It proves the sole application of LAS based generator is useless.
- c) The uncertainty of the most probable result has been largely reduced to 4.58% in the case study, which may reflect that the proposed generator can be best applied in a large scale of fluctuation scenario.
- d) The conditional random field generator can simulate the range of a CPT profile. For example, with two conducted CPTs respectively on the two sides of a problem domain, the maximal and minimal boundary of the CPT profile at the central position within this domain can be simulated. The real profile must be inside those two boundaries, which can be used to verify the reliability of conducted CPTs. In particular, the distribution of the profile of the normalized friction ratio has a COV of 0.235 and the distribution of the profile of the normalized cone resistance has a COV of 0.313.

Reference

- Anagnostopoulos, A., Koukis, G., Sabatakakis, N., & Tsiambaos, G. (2003). Empirical correlations of soil parameters based on Cone Penetration Tests (CPT) for Greek soils. *Geotechnical And Geological Engineering*, 21(4), 377-387. doi: 10.1023/b:gege.0000006064.47819.1a
- Chessa, A. (2006). A Markov Chain Model for Subsurface Characterization: Theory and Applications. *Mathematical Geology*, 38(4), 503-505. doi: 10.1007/s11004-006-9037-9
- Cone penetration test - Wikipedia. (2022). Retrieved 19 September 2022, from https://en.wikipedia.org/wiki/Cone_penetration_test
- Campanella, R.G., Gillespie, D., Robertson, P.K., 1982. Pore pressures during cone penetration testing. In: Proceedings of the 2nd European Symposium on Penetration Testing, vol. 2, pp. 507e512. ESOPT-2, Amsterdam.
- Clayton, C. (2001). *Managing geotechnical risk*. London: Telford.
- Griffiths, D. V., Huang, J., & Fenton, G. A. (2015). Probabilistic slope stability analysis using RFEM with non-stationary random fields. In *Geotechnical safety and risk V* (pp. 704-709). IOS Press.
- Fenton, G., & Griffiths, D. (2007). Random Field Generation and the Local Average Subdivision Method. *CISM Courses And Lectures*, 201-223. doi: 10.1007/978-3-211-73366-0_9
- Fenton, G., & Griffiths, D. (2008). *Risk assessment in geotechnical engineering*. Hoboken: Wiley.
- Fenton, G., & Vanmarcke, E. (1990). Simulation of Random Fields via Local Average Subdivision. *Journal Of Engineering Mechanics*, 116(8), 1733-1749. doi: 10.1061/(asce)0733-9399(1990)116:8(1733)
- Hernández-Lemus, E. (2021). Random Fields in Physics, Biology and Data Science. *Frontiers In Physics*, 9. doi: 10.3389/fphy.2021.641859
- Hicks, M. (2009). *Risk and variability in geotechnical engineering*. London: Thomas Telford Ltd.
- Hu, Y., & Wang, Y. (2020). Probabilistic soil classification and stratification in a vertical cross-section from limited cone penetration tests using random field and Monte Carlo simulation. *Computers And Geotechnics*, 124, 103634. doi: 10.1016/j.compgeo.2020.103634
- Jamshidi Chenari, R., & Kamyab Farahbakhsh, H. (2015). Generating non-stationary random fields of auto-correlated, normally distributed CPT profile by matrix decomposition method. *Georisk: Assessment And Management Of Risk For Engineered Systems And Geohazards*, 9(2), 96-108. doi: 10.1080/17499518.2015.1033429
- Liu, Y., Li, J., Sun, S., & Yu, B. (2019). Advances in Gaussian random field generation: a review. *Computational Geosciences*, 23(5), 1011-1047. doi: 10.1007/s10596-019-09867-y

- Lloret-Cabot, M., Hicks, M., & van den Eijnden, A. (2012). Investigation of the reduction in uncertainty due to soil variability when conditioning a random field using Kriging. *Géotechnique Letters*, 2(3), 123-127. doi: 10.1680/geolett.12.00022
- McGann, C., Bradley, B., Taylor, M., Wotherspoon, L., & Cubrinovski, M. (2015). Development of an empirical correlation for predicting shear wave velocity of Christchurch soils from cone penetration test data. *Soil Dynamics And Earthquake Engineering*, 75, 66-75. doi: 10.1016/j.soildyn.2015.03.023
- Montoya-Noguera, S., Zhao, T., Hu, Y., Wang, Y., & Phoon, K. (2019). Simulation of non-stationary non-Gaussian random fields from sparse measurements using Bayesian compressive sampling and Karhunen-Loève expansion. *Structural Safety*, 79, 66-79. doi: 10.1016/j.strusafe.2019.03.006
- Ramsey, N. (2010). Some issues related to applications of the CPT. 2nd International Symposium on Cone Penetration Testing, CA, USA
- Robertson, P. (2010). Soil behaviour type from the CPT: an update. 2nd International Symposium on Cone Penetration Testing, CA, USA
- Robertson, P. (2015). Soil behavior type using the DMT. Gregg Drilling & Testing Inc., Signal Hill, CA, USA.
- Robertson, P. (1990). Soil classification using the cone penetration test. *Canadian Geotechnical Journal*, 27(1), 151-158. doi: 10.1139/t90-014
- Robertson, P., & Wride, C. (1998). Evaluating cyclic liquefaction potential using the cone penetration test. *Canadian Geotechnical Journal*, 35(3), 442-459. doi: 10.1139/t98-017
- Shi, C., & Wang, Y. (2021a). Development of Subsurface Geological Cross-Section from Limited Site-Specific Boreholes and Prior Geological Knowledge Using Iterative Convolution XGBoost. *Journal Of Geotechnical And Geoenvironmental Engineering*, 147(9). doi: 10.1061/(asce)gt.1943-5606.0002583
- Shi, C., & Wang, Y. (2021b). Nonparametric and data-driven interpolation of subsurface soil stratigraphy from limited data using multiple point statistics. *Canadian Geotechnical Journal*, 58(2), 261-280. doi: 10.1139/cgj-2019-0843
- Tillmann, A., Englert, A., Nyari, Z., Fejes, I., Vanderborght, J., & Vereecken, H. (2008). Characterization of subsoil heterogeneity, estimation of grain size distribution and hydraulic conductivity at the Krauthausen test site using Cone Penetration Test. *Journal Of Contaminant Hydrology*, 95(1-2), 57-75. doi: 10.1016/j.jconhyd.2007.07.013
- Wang, X., Wang, H., & Liang, R. (2017). A method for slope stability analysis considering subsurface stratigraphic uncertainty. *Landslides*, 15(5), 925-936. doi: 10.1007/s10346-017-0925-5

Wang, Y., Huang, K., & Cao, Z. (2013). Probabilistic identification of underground soil stratification using cone penetration tests. *Canadian Geotechnical Journal*, 50(7), 766-776. doi: 10.1139/cgj-2013-0004

Xiao, T., Zhang, L., Li, X., & Li, D. (2017). Probabilistic Stratification Modeling in Geotechnical Site Characterization. *ASCE-ASME Journal Of Risk And Uncertainty In Engineering Systems, Part A: Civil Engineering*, 3(4). doi: 10.1061/ajrua6.0000924

Appendices: Python Codes

Appendix A: Main process

```
1. import numpy as np
2. import matplotlib.pyplot as plt
3. import robertson_new as Frob_new
4. import Additional_subroutines as subs
5. from shutil import copyfile
6. import pandas as pd
7. from numpy.ma import sin, cos, exp, log
8. from scipy.stats import norm
9.
10. '-----Process the result file including fr and qc to classify-----'
11. #Read the fr and qc for all realizations in the feild.RES file
12. list1 = []
13. list2 = []
14. with open("field_co.RES", "r") as f:
15.     lines = f.readlines()
16.     for line in lines:
17.         a = line.split()
18.         x = a[0]
19.         y = a[1]
20.         list1.append(x)
21.         list2.append(y)
22.
23. for i in range(len(list1)):
24.     list1[i] = float(list1[i])
25. for i in range(len(list2)):
26.     list2[i] = float(list2[i])
27.
28. nfr = np.array(list1).reshape(-1, 1) #Generated log normalized friction ratio
29. nqt = np.array(list2).reshape(-1, 1) #Generated log normalized tip resistance
30.
31.
32. #Read the number and size of cells in both directions
33. lines = open("input.DAT").read().splitlines()
34. no_cell = lines[1].split()
35. no_cell_h = float(no_cell[0])
36. no_cell_v = float(no_cell[1])
37. cell_size = lines[2].split()
38. cell_size_vh = float(cell_size[1])
39. cell_oneR = int(no_cell_h * no_cell_v)
40. realizations = int(lines[0])
41.
42. thickness = np.ones(nfr.shape) * cell_size_vh #Actually useless and it won't effect the result
43. matrix_generalized = np.hstack((thickness, nqt, nfr))
44.
45. polygons = Frob_new.plot_Robertson(matrix_generalized)
46. matrix_final = Frob_new.deterministic(matrix_generalized, polygons)
47. classification_final = matrix_final[:, 1]
48. classification_eachR = np.array_split(classification_final, realizations)
49.
50. '-----Create .VTK files which can be shown in Paraview-----'
51. name = 1
52.
53. for i in range(int(realizations)):
54.     i_str = str(name)
55.     filename = 'realization' + i_str + '.vtk'
56.     file = open(filename, 'a')
57.     copyfile('Example.vtk', filename)
```

```
58. file.write('\r')
59.
60. for ii in classification_eachR[i]:
61.     file.write(str(ii)+'\r')
62. file.close()
63. name = name + 1
```

Appendix B: Determination of the number of realizations

```
1. import numpy as np
2. import Additional_subroutines as subs
3. import os
4. import robertson_new as Frob_new
5. import matplotlib.pyplot as plt
6.
7. realizations = np.linspace(10, 100, 5)
8. realizations_additional = realizations + 10
9.
10. unce_ave1 = np.zeros(realizations.shape)
11. unce_ave2 = np.zeros(realizations_additional.shape)
12.
13. for ii, r in enumerate(realizations):
14.     # Create a temporary .dat file to store modified values
15.     lines = open('input.dat').read().splitlines()
16.     lines[0] = "%6.0F"%(r)
17.     open('input.dat', 'w').write('\n'.join(lines))
18.     #Run analysis
19.     os.system(r"@echo | ConditionalRandomFieldGenerator.exe")
20.
21.     #open the result file and read the generated qc and rf
22.     list1 = []
23.     list2 = []
24.     with open("field_co.RES", "r") as f:
25.         lines = f.readlines()
26.         for line in lines:
27.             a = line.split()
28.             x = a[0]
29.             y = a[1]
30.             list1.append(x)
31.             list2.append(y)
32.
33.     for i in range(len(list1)):
34.         list1[i] = float(list1[i])
35.     for i in range(len(list2)):
36.         list2[i] = float(list2[i])
37.
38.     nfr = np.array(list1).reshape(-1, 1) #Generated log normalized friction ratio
39.     nqt = np.array(list2).reshape(-1, 1) #Generated log normalized tip resistance
40.
41.     #Read the number and size of cells in both directions
42.     lines = open('input.DAT').read().splitlines()
43.     no_cell = lines[1].split()
44.     no_cell_h = float(no_cell[0])
45.     no_cell_v = float(no_cell[1])
46.     cell_size = lines[2].split()
47.     cell_size_vh = float(cell_size[1])
48.
49.     thickness = np.ones(nfr.shape) * cell_size_vh #Actually useless and it won't effect the result
50.     matrix_generalized = np.hstack((thickness, nqt, nfr))
51.
52.     polygons = Frob_new.plot_Robertson(matrix_generalized)
53.     matrix_final = Frob_new.deterministic(matrix_generalized, polygons)
54.     classification_final = matrix_final[:, 1]
55.
56.     cell_oneR = int(no_cell_h * no_cell_v)
57.     r_changing = int(len(classification_final)/cell_oneR)
58.     unce_ave1[ii] = subs.FindAveUnce(classification_final, cell_oneR, r_changing)
59.
```

```

60.
61. for ii, r in enumerate(realizations_additional):
62.     # Create a temporary .dat file to store modified values
63.     lines = open('input.dat').read().splitlines()
64.     lines[0] = '%6.0f'%(r)
65.     open('input.dat', 'w').write('\n'.join(lines))
66.     #Run analysis
67.     os.system(r'@echo | ConditionalRandomFieldGenerator.exe')
68.
69.     #open the result file and read the generated qc and rf
70.     list1 = []
71.     list2 = []
72.     with open("field_co.RES", "r") as f:
73.         lines = f.readlines()
74.         for line in lines:
75.             a = line.split()
76.             x = a[0]
77.             y = a[1]
78.             list1.append(x)
79.             list2.append(y)
80.
81.     for i in range(len(list1)):
82.         list1[i] = float(list1[i])
83.     for i in range(len(list2)):
84.         list2[i] = float(list2[i])
85.
86.     nfr = np.array(list1).reshape(-1, 1) #Generated log normalized friction ratio
87.     nqt = np.array(list2).reshape(-1, 1) #Generated log normalized tip resistance
88.
89.     #Read the number and size of cells in both directions
90.     lines = open('input.DAT').read().splitlines()
91.     no_cell = lines[1].split()
92.     no_cell_h = float(no_cell[0])
93.     no_cell_v = float(no_cell[1])
94.     cell_size = lines[2].split()
95.     cell_size_vh = float(cell_size[1])
96.
97.     thickness = np.ones(nfr.shape) * cell_size_vh #Actually useless and it won't effect the result
98.     matrix_generalized = np.hstack((thickness, nqt, nfr))
99.
100.    polygons = Frob_new.plot_Robertson(matrix_generalized)
101.    matrix_final = Frob_new.deterministic(matrix_generalized, polygons)
102.    classification_final = matrix_final[:, 1]
103.
104.    cell_oneR = int(no_cell_h * no_cell_v)
105.    r_changing = int(len(classification_final)/cell_oneR)
106.    unce_ave2[ii] = subs.FindAveUnce(classification_final, cell_oneR, r_changing)
107.
108.    Change_over_realizations = abs(unce_ave1 - unce_ave2) / unce_ave1
109.    plt.figure()
110.    plt.plot(realizations, Change_over_realizations)
111.    plt.xlabel('The number of realizations')
112.    plt.ylabel('Percent change in the uncertainty of the most probable result')

```

Appendix C1: Determination of the most probable result and its uncertainty

```
1. import Additional_subroutines as subs
2.
3. '-----Most probable result for classifications and its uncertainty-----'
4. #To get the most probable result
5. most_probable = subs.MostProbableResult(classification_final, cell_oneR, realizations, 'example.vtk')
6.
7. #To get the uncertainty of the most probable result
8. prob_most_probable = subs.FindUncertainty(classification_final, cell_oneR, realizations, 'example.vtk')
9.
10. #To get the average uncertainty
11. ave_uncertainty = subs.FindAveUnce(classification_final, cell_oneR, realizations)
12. print(ave_uncertainty)
```

Appendix C2: Determination of the most probable result and its uncertainty (Additional subroutines)

```
1. import numpy as np
2. from collections import Counter
3. from shutil import copyfile
4.
5. def Classification_SameCell(classification_allR, no_cell_oneR, no_realization):
6.     period = no_cell_oneR
7.     length = no_realization
8.     list_class_SameCell = []
9.
10.    for i in range(period):
11.        position = i
12.        extract = np.zeros(length)
13.        for ii in range(length):
14.            extract[ii] = classification_allR[position]
15.            position += period
16.
17.        list_class_SameCell.append(extract)
18.
19.    return list_class_SameCell
20.
21. #To get the probability of the most probable classification in each cell
22. def FindUncertainty(classification_allR, no_cell_oneR, no_realization, exampleVTK):
23.     class_SameCell = Classification_SameCell(classification_allR, no_cell_oneR, no_realization)
24.     prob_eachcell = []
25.
26.     for i in range(len(class_SameCell)):
27.         a = Counter(class_SameCell[i]).most_common(1)[0][0]
28.         #print(a)
29.         n = 0
30.
31.         for ii in range(len(class_SameCell[i])):
32.             if class_SameCell[i][ii] == a:
33.                 n += 1
34.         prob = n/len(class_SameCell[i])
35.
36.         prob_eachcell.append(prob)
37.
38.     uncertainty_eachcell = 1 - np.array(prob_eachcell)
39.
40.     filename = 'The uncertainty of the most probable result.vtk'
41.
42.     file = open(filename, 'a')
43.     copyfile(exampleVTK, filename)
44.     file.write('\r')
45.
46.     for ii in uncertainty_eachcell:
47.         file.write(str(ii)+'\r')
48.     file.close()
49.     return uncertainty_eachcell
50.
51. def MostProbableResult(classification_allR, no_cell_oneR, no_realization, exampleVTK):
52.     class_SameCell = Classification_SameCell(classification_allR, no_cell_oneR, no_realization)
53.     mostprobable = np.zeros(no_cell_oneR)
54.     for i in range(len(class_SameCell)):
55.         a = Counter(class_SameCell[i]).most_common(1)[0][0]
56.         mostprobable[i] = a
57.
```



```

58. filename = 'Most probable result.vtk'
59.
60. file = open(filename, 'a')
61. copyfile(exampleVTK, filename)
62. file.write('\r')
63.
64. for ii in mostprobable:
65.     file.write(str(ii)+'\r')
66. file.close()
67.
68. return mostprobable
69.
70. def MostProbableResult_Array(classification_allR, no_cell_oneR, no_realization):
71.     class_SameCell = Classification_SameCell(classification_allR, no_cell_oneR, no_realization)
72.     mostprobable_array = np.zeros(no_cell_oneR)
73.     for i in range(len(class_SameCell)):
74.         a = Counter(class_SameCell[i]).most_common(1)[0][0]
75.         mostprobable_array[i] = a
76.     return mostprobable_array
77.
78. def FindAveUnce(classification_allR, no_cell_oneR, no_realization):
79.     class_SameCell = Classification_SameCell(classification_allR, no_cell_oneR, no_realization)
80.     prob_eachcell = []
81.
82.     for i in range(len(class_SameCell)):
83.         a = Counter(class_SameCell[i]).most_common(1)[0][0]
84.         #print(a)
85.         n = 0
86.
87.         for ii in range(len(class_SameCell[i])):
88.             if class_SameCell[i][ii] == a:
89.                 n += 1
90.         prob = n/len(class_SameCell[i])
91.
92.         prob_eachcell.append(prob)
93.
94.     uncertainty_eachcell = 1 - np.array(prob_eachcell)
95.
96.     unce_ave = np.mean(uncertainty_eachcell)
97.
98.     return unce_ave

```

Appendix D1: Determination of statistics of case study (mean and standard deviation)

```
1. import numpy as np
2. import pandas as pd
3. import matplotlib.pyplot as plt
4. from shutil import copyfile
5. from numpy import polyfit, poly1d
6. from numpy.ma import sin, cos, exp, log
7.
8. '-----Read the results after using the CPT reading scrip-----'
9. df81 = pd.read_excel('CPT81_FindStatistics.xlsx')
10. depth81 = -df81.values[:, 0]
11. qt81 = df81.values[0:, 1]
12. fs81 = df81.values[:, 2]
13. sigv81 = df81.values[:, 5]
14. sigv_eff81 = df81.values[:, 6]
15. nqt81 = (qt81 - sigv81)/sigv_eff81
16. nfr81 = (fs81*100)/(qt81 - sigv81)
17. log_nqt81 = np.log(nqt81)
18. log_nfr81 = np.log(nfr81)
19.
20. df82 = pd.read_excel('CPT82_FindStatistics.xlsx')
21. depth82 = -df82.values[:, 0]
22. qt82 = df82.values[0:, 1]
23. fs82 = df82.values[:, 2]
24. sigv82 = df82.values[:, 5]
25. sigv_eff82 = df82.values[:, 6]
26. nqt82 = (qt82 - sigv82)/sigv_eff82
27. nfr82 = (fs82*100)/(qt82 - sigv82)
28. log_nqt82 = np.log(nqt82)
29. log_nfr82 = np.log(nfr82)
30.
31. df85 = pd.read_excel('CPT85_FindStatistics.xlsx')
32. depth85 = -df85.values[:, 0]
33. qt85 = df85.values[0:, 1]
34. fs85 = df85.values[:, 2]
35. sigv85 = df85.values[:, 5]
36. sigv_eff85 = df85.values[:, 6]
37. nqt85 = (qt85 - sigv85)/sigv_eff85
38. nfr85 = (fs85*100)/(qt85 - sigv85)
39. log_nqt85 = np.log(nqt85)
40. log_nfr85 = np.log(nfr85)
41.
42. log_nfr81 = np.round(log_nfr81, 3)
43. log_nfr82 = np.round(log_nfr82, 3)
44. log_nfr85 = np.round(log_nfr85, 3)
45.
46. log_nqt81 = np.round(log_nqt81, 3)
47. log_nqt82 = np.round(log_nqt82, 3)
48. log_nqt85 = np.round(log_nqt85, 3)
49.
50. '-----To get the mean, std and scale of fluctuation for the input of random field-----'
51. 'To get the mean'
52. meanfr_log_norm = np.mean((log_nfr81, log_nfr82, log_nfr85))
53. meanqt_log_norm = np.mean((log_nqt81, log_nqt82, log_nqt85))
54.
55. 'To get the std'
56. stdfr_81 = np.std(log_nfr81)
57. stdfr_82 = np.std(log_nfr82)
```

```
58. stdfr_85 = np.std(log_nfr85)
59. stdfr = (stdfr_81 + stdfr_82 + stdfr_85) / 3
60.
61. stdqt_81 = np.std(log_nqt81)
62. stdqt_82 = np.std(log_nqt82)
63. stdqt_85 = np.std(log_nqt85)
64. stdqt = (stdqt_81 + stdqt_82 + stdqt_85) / 3
```

Appendix D2: Determination of statistics of case study (scale of fluctuation)

```
1. 'To get the scale of fluctuation'
2. #Remove some abnormal values
3. nqt81 = nqt81[9:-1]
4. nfr81 = nfr81[9:-1]
5. nqt82 = nqt82[9:-1]
6. nfr82 = nfr82[9:-1]
7. nqt85 = nqt85[9:-1]
8. nfr85 = nfr85[9:-1]
9.
10. depth81 = depth81[9:-1]
11. depth82 = depth82[9:-1]
12. depth85 = depth85[9:-1]
13.
14. '-----Get theta from normalized cone resistance-----'
15. ##-----For normalized qt-----
16. ####Remove the trend first
17. ##To get the regression function of the fr/qc
18. depth_total = np.hstack((depth81,depth82, depth85)) #the depth now is negative
19. nqt_total = np.hstack((nqt81, nqt82, nqt85))
20.
21. plt.figure()
22. plt.plot(nqt_total , depth_total, 'rx', label = 'data')
23. plt.xlabel('fr [-]')
24. plt.ylabel('depth [m]')
25.
26. coeff = polyfit(-depth_total, nqt_total, 1)
27. x = -depth81
28. y = coeff[0]*x + coeff[1]
29. plt.plot(y, -x, label = 'regression')
30. plt.legend()
31. plt.show()
32.
33. nqt_regression = y
34.
35. ##Get the standard deviation from the detrended values
36. eps81 = nqt81 - nqt_regression
37. eps82 = nqt82 - nqt_regression
38. eps85 = nqt85 - nqt_regression
39. eps_total = np.hstack((eps81, eps82, eps85))
40. n_std_square = 0.0
41.
42. plt.figure()
43. plt.plot(eps82, -depth82)
44.
45. ##The detrended nqt
46. nqt_detrended = (eps81 + eps82 + eps85)/3
47. print('mean(nqt_detrended):', np.mean(nqt_detrended))##Show the detrended values have a mean of 0
48.
49. for eps in eps_total:
50.     n_std_square += (eps - np.mean(nqt_detrended))**2
51. std_detrended_nqt = (n_std_square/len(eps_total))**0.5
52.
53. print('std_detrended_nqt:', std_detrended_nqt)
54.
55. ##Convert the detrended values to uniform distribution
56. nqt_unifrom = nqt_detrended/std_detrended_nqt
57. test_std = np.std(nqt_unifrom)
58. print('test_std:', test_std) ##Show that now nqt is uniform distribution and std is 1
59. ## Plot the experimental correlation function
```

```

60. ##There are two key points for the correlation function
61. ##1. The minimal deltaz is chosen as the minimal thickness in the CPT reading script.
   The following deltazs are the interger multiples of minimal deltaz
62. ##2. In order to extract all the available pairs in the profile, the initila depth can be all depths in the profile.
63. standard_depth = -depth81
64. standard_depth = np.round(standard_depth, 2)
65. qt_toGetTheta = nqt_unifrom
66.
67. list_rho_all = [1]
68. deltaz_index = np.linspace(0, 50, 51)
69.
70. for i in deltaz_index:
71.
72.     deltaz = (i + 1)*0.12
73.     ndeltaz = 0
74.     z_sum_deltaz = deltaz
75.
76.     list_qt_z = []
77.     list_qt_z_sum_deltaz = []
78.     list_z = []
79.     list_z_sum_deltaz = []
80.
81.     for ii in standard_depth:
82.         initial_depth = ii
83.         z_sum_deltaz = (initial_depth + deltaz).round(2)
84.
85.         z_sum_deltaz_GETd = z_sum_deltaz
86.
87.         for iii in range(300):
88.             if z_sum_deltaz_GETd <= max(standard_depth) and z_sum_deltaz_GETd not in list_z_sum_deltaz:
89.                 ndeltaz += 1
90.                 list_z_sum_deltaz.append(z_sum_deltaz_GETd.round(2))
91.
92.                 z_sum_deltaz_GETd += deltaz
93.                 z_sum_deltaz_GETd = z_sum_deltaz_GETd.round(2)
94.
95.         for iv in range(len(list_z_sum_deltaz)):
96.
97.             #To get the index of z+deltaz and the corresponding fr
98.             index_z_sum_deltaz = np.where(standard_depth == list_z_sum_deltaz[iv])
99.             list_qt_z_sum_deltaz.append(qt_toGetTheta[index_z_sum_deltaz])
100.
101.             #To get the index for the z and the corresponding fr
102.             array_z_sum_deltaz = np.array(list_z_sum_deltaz)
103.             array_z = array_z_sum_deltaz - deltaz
104.             array_z = np.round(array_z, 2)
105.             list_z = list(array_z)
106.
107.             index_z = np.where(standard_depth == list_z[iv])
108.             list_qt_z.append(qt_toGetTheta[index_z])
109.
110.             rho_deltaz = sum(np.array(list_qt_z) * np.array(list_qt_z_sum_deltaz))/ ndeltaz
111.             #rho_deltaz = rho_deltaz[0]
112.
113.             list_rho_all.append(rho_deltaz)
114. array_deltaz_all = np.linspace(0, 51*0.12, 52)
115. list_deltaz_all = list(array_deltaz_all)
116.
117. plt.figure()
118. plt.plot(list_deltaz_all, list_rho_all, linestyle = '--', label = 'rho(deltaz)')
119. plt.xlabel('deltaz [m]')

```

```

120. plt.ylabel('experimental correlation function rho_qt [-]')
121. plt.title('Correlation function to find thetav')
122.
123.
124. #Fit a theoretical Markov correlation function
125. theta = np.array([0.1, 1/4, 1/2, 1, 2, 3, 4])
126. deltaz_markov = np.linspace(0, 6, 100)
127. for i in range(len(theta)):
128.     roum = exp(-2*deltaz_markov/theta[i])
129.     plt.plot(deltaz_markov, roum, label = f'theta = {theta[i]}')
130. plt.legend()
131. plt.show()
132. '-----Do the same thing to friction ratio-----'
133. depth_total = np.hstack((depth81,depth82, depth85)) #the depth now is negative
134. nfr_total = np.hstack((nfr81, nfr82, nfr85)) #the fr has been detrended
135.
136. plt.figure()
137. plt.plot(nfr_total, depth_total, 'rx', label = 'data')
138. plt.xlabel('fr [-]')
139. plt.ylabel('depth [m]')
140.
141. coeff = polyfit(-depth_total, nfr_total, 1)
142. x = -depth81
143. y = coeff[0]*x + coeff[1]
144. plt.plot(y, -x, label = 'regression')
145. plt.legend()
146. plt.show()
147.
148. nfr_regression = y
149.
150. ##Get the standard devaition from the detrended values
151. eps81 = nfr81 - nfr_regression
152. eps82 = nfr82 - nfr_regression
153. eps85 = nfr85 - nfr_regression
154. eps_total = np.hstack((eps81, eps82, eps85))
155. n_std_square = 0.0
156.
157. plt.figure()
158. plt.plot(eps82, -depth82)
159.
160. ##The detrended nfr
161. nfr_detrended = (eps81 + eps82 + eps85)/3
162. print('mean(nfr_detrended):', np.mean(nfr_detrended))##Show the detrended values have a mean of 1
163.
164. for eps in eps_total:
165.     n_std_square += (eps - 0)**2
166. std_detrended_nfr = (n_std_square/len(eps_total))**0.5
167.
168. print('std_detrended_nfr:', std_detrended_nfr)
169.
170. ##Convert the detrended values to uniform distribution
171. nfr_unifrom = nfr_detrended/std_detrended_nfr
172. test_std = np.std(nfr_unifrom)
173. print('test_std:', test_std)
174.
175.
176. # Plot the experimental correlation function
177. standard_depth = -depth81
178. standard_depth = np.round(standard_depth, 2)
179. fr_toGetTheta = nfr_unifrom
180.

```

```

181. list_rho_all = [1]
182. deltaz_index = np.linspace(0, 50, 51)
183.
184. for i in deltaz_index:
185.
186.     deltaz = (i + 1)*0.12
187.     ndeltaz = 0
188.     z_sum_deltaz = deltaz
189.
190.     list_fr_z = []
191.     list_fr_z_sum_deltaz = []
192.     list_z = []
193.     list_z_sum_deltaz = []
194.
195.     for ii in standard_depth:
196.         initial_depth = ii
197.         z_sum_deltaz = (initial_depth + deltaz).round(2)
198.
199.         z_sum_deltaz_GETd = z_sum_deltaz
200.
201.         for iii in range(300):
202.             if z_sum_deltaz_GETd <= max(standard_depth) and z_sum_deltaz_GETd not in list_z_sum_deltaz:
203.                 ndeltaz += 1
204.                 list_z_sum_deltaz.append(z_sum_deltaz_GETd.round(2))
205.
206.                 z_sum_deltaz_GETd += deltaz
207.                 z_sum_deltaz_GETd = z_sum_deltaz_GETd.round(2)
208.
209.         for iv in range(len(list_z_sum_deltaz)):
210.
211.             #To get the index of z+deltaz and the corresponding fr
212.             index_z_sum_deltaz = np.where(standard_depth == list_z_sum_deltaz[iv])
213.             list_fr_z_sum_deltaz.append(fr_toGetTheta[index_z_sum_deltaz])
214.
215.             #To get the index for the z and the corresponding fr
216.             array_z_sum_deltaz = np.array(list_z_sum_deltaz)
217.             array_z = array_z_sum_deltaz - deltaz
218.             array_z = np.round(array_z, 2)
219.             list_z = list(array_z)
220.
221.             index_z = np.where(standard_depth == list_z[iv])
222.             list_fr_z.append(fr_toGetTheta[index_z])
223.
224.             rho_deltaz = sum(np.array(list_fr_z) * np.array(list_fr_z_sum_deltaz))/ ndeltaz
225.             #rho_deltaz = rho_deltaz[0]
226.
227.             list_rho_all.append(rho_deltaz)
228.
229. array_deltaz_all = np.linspace(0, 51*0.12, 52)
230. list_deltaz_all = list(array_deltaz_all)
231.
232. plt.figure()
233. plt.plot(list_deltaz_all, list_rho_all, linestyle = '--', label = 'rho(deltaz)')
234. plt.xlabel('deltaz [m]')
235. plt.ylabel('experimental correlation function rho_fr [-]')
236. plt.title('Correlation function to find thetav')
237.
238.
239. #Fit a theoretical Markov correlation function
240. theta = np.array([0.1, 1/4, 1/2, 1, 2, 3, 4])
241. deltaz_markov = np.linspace(0, 6, 100)

```

```
242. for i in range(len(theta)):
243.     roun = exp(-2*deltaz_markov/theta[i])
244.     plt.plot(deltaz_markov, roun, label = f'theta = {theta[i]')
245. plt.legend()
246. plt.show()
```


Appendix E: Investigation in one less CPT situation

```
1. import numpy as np
2. import matplotlib.pyplot as plt
3. import robertson_new as Frob_new
4. import Additional_subroutines as subs
5. from shutil import copyfile
6. import pandas as pd
7. from numpy.ma import sin, cos, exp, log
8. from scipy.stats import norm
9.
10. '-----Process the result file including fr and qc to classify-----'
11. #Read the fr and qc for all realizations in the feild.RES file
12. list1 = []
13. list2 = []
14. with open("field_co.RES", "r") as f:
15.     lines = f.readlines()
16.     for line in lines:
17.         a = line.split()
18.         x = a[0]
19.         y = a[1]
20.         list1.append(x)
21.         list2.append(y)
22.
23. for i in range(len(list1)):
24.     list1[i] = float(list1[i])
25. for i in range(len(list2)):
26.     list2[i] = float(list2[i])
27.
28. nfr = np.array(list1).reshape(-1, 1) #Generated log normalized friction ratio
29. nqt = np.array(list2).reshape(-1, 1) #Generated log normalized tip resistance
30.
31.
32. #Read the number and size of cells in both directions
33. lines = open('input.DAT').read().splitlines()
34. no_cell = lines[1].split()
35. no_cell_h = float(no_cell[0])
36. no_cell_v = float(no_cell[1])
37. cell_size = lines[2].split()
38. cell_size_vh = float(cell_size[1])
39. cell_oneR = int(no_cell_h * no_cell_v)
40. realizations = int(lines[0])
41. '-----Compare the middle column in terms of classifications-----'
42. ##Extract the middle column and compare
43. mostprobable_array = subs.MostProbableResult_Array(classification_final, cell_oneR, realizations)
44. middlecolumn = []
45.
46. middle_index = 48
47. for i in range(int(no_cell_v)):
48.     middlecolumn.append(mostprobable_array[int(middle_index)])
49.     middle_index += no_cell_h
50.
51. ##write in VTK file to visualize
52. filename = 'middlecolumn.vtk'
53. file = open(filename, 'a')
54. copyfile('ClassificationExample.vtk', filename)
55. file.write('\r')
56.
57. for i in middlecolumn:
58.     file.write(str(i)+'\r')
59. file.close()
```

```

60.
61. ##read the actual CPT1 and compare the difference
62. real_CPT = []
63. with open('CPT81_classification.dat', 'r') as f:
64.     lines = f.readlines()
65.     for line in lines:
66.         CPT1_classification = float(line)
67.         real_CPT.append(CPT1_classification)
68.
69. n = 0
70. for ii in range(len(real_CPT)):
71.     if middlecolumn[ii] != real_CPT[ii]:
72.         n += 1
73. Percent_diff = n/len(real_CPT)
74.
75. '-----Compare the middle column in terms of fr and qt-----'
76. ##Get the log_nqt and log_nfr for each realization
77. log_nqt_eachR = np.array_split(nqt, realizations)
78. log_nfr_eachR = np.array_split(nfr, realizations)
79. ##Get the middle column for each realization, stored in list
80. middlecolumn_lognqt = []
81. middlecolumn_lognfr = []
82.
83. ##First for log_nqt
84. for i in range(realizations):
85.     middlecolumn_qtcontainer = np.zeros(int(no_cell_v))
86.     middle_index = 48
87.     for ii in range(int(no_cell_v)):
88.         middlecolumn_qtcontainer[ii] = log_nqt_eachR[i][int(middle_index)]
89.         middle_index += no_cell_h
90.     middlecolumn_lognqt.append(middlecolumn_qtcontainer)
91.
92. ##Second for log_nfr
93. for i in range(realizations):
94.     middlecolumn_frcontainer = np.zeros(int(no_cell_v))
95.     middle_index = 48
96.     for ii in range(int(no_cell_v)):
97.         middlecolumn_frcontainer[ii] = log_nfr_eachR[i][int(middle_index)]
98.         middle_index += no_cell_h
99.     middlecolumn_lognfr.append(middlecolumn_frcontainer)
100.
101. ##Get normalized qt and normalized fr at the same cell for each realization
102. middleC_nqt_eachR = []
103. middleC_nfr_eachR = []
104.
105. for i in range(int(no_cell_v)):
106.     nqtcontainer_realizations = np.zeros(realizations)
107.     for ii in range(realizations):
108.         nqtcontainer_realizations[ii] = exp(middlecolumn_lognqt[ii][i]) ##Notice the exponential Func
109.     middleC_nqt_eachR.append(nqtcontainer_realizations)
110.
111. for i in range(int(no_cell_v)):
112.     nfrcontainer_realizations = np.zeros(realizations)
113.     for ii in range(realizations):
114.         nfrcontainer_realizations[ii] = exp(middlecolumn_lognfr[ii][i]) ##Notice the exponential Func
115.     middleC_nfr_eachR.append(nfrcontainer_realizations)
116.
117. ##mean for nqt and nfr
118. mean_eachC_nqt = []
119. for i in range(int(no_cell_v)):
120.     mean_tem = np.mean(middleC_nqt_eachR[i])

```

```

121. mean_eachC_nqt.append(mean_tem)
122.
123. mean_eachC_nfr = []
124. for i in range(int(no_cell_v)):
125.     mean_tem = np.mean(middleC_nfr_eachR[i])
126.     mean_eachC_nfr.append(mean_tem)
127.
128. #std for nqt and nfr
129. std_eachC_nqt = []
130. for i in range(int(no_cell_v)):
131.     std_tem = np.std(middleC_nqt_eachR[i])
132.     std_eachC_nqt.append(std_tem)
133.
134. std_eachC_nfr = []
135. for i in range(int(no_cell_v)):
136.     std_tem = np.std(middleC_nfr_eachR[i])
137.     std_eachC_nfr.append(std_tem)
138.
139. ##The final version of the mean and std are the average values over depth
140. final_mean_middleC_nqt = sum(mean_eachC_nqt)/(len(mean_eachC_nqt))
141. final_mean_middleC_nfr = sum(mean_eachC_nfr)/(len(mean_eachC_nfr))
142.
143. final_std_middleC_nqt = sum(std_eachC_nqt)/(len(std_eachC_nqt))
144. final_std_middleC_nfr = sum(std_eachC_nfr)/(len(std_eachC_nfr))
145.
146.
147. ##-----Plot the simulated range and measured CPT-----##
148.
149. ##Get the max and min values to get the range plot
150. max_middleC_nqt = []
151. for i in range(int(no_cell_v)):
152.     max_tem = np.max(middleC_nqt_eachR[i])
153.     max_middleC_nqt.append(max_tem)
154.
155. max_middleC_nfr = []
156. for i in range(int(no_cell_v)):
157.     max_tem = np.max(middleC_nfr_eachR[i])
158.     max_middleC_nfr.append(max_tem)
159.
160.
161. min_middleC_nqt = []
162. for i in range(int(no_cell_v)):
163.     min_tem = np.min(middleC_nqt_eachR[i])
164.     min_middleC_nqt.append(min_tem)
165.
166. min_middleC_nfr = []
167. for i in range(int(no_cell_v)):
168.     min_tem = np.min(middleC_nfr_eachR[i])
169.     min_middleC_nfr.append(min_tem)
170.
171. #####The pdf based on the above mean and standard deviation#####
172. plt.figure()
173. x_axis_nqt = np.linspace(min(min_middleC_nqt), max(max_middleC_nqt), 100)
174. plt.plot(x_axis_nqt, norm.pdf(x_axis_nqt, final_mean_middleC_nqt, final_std_middleC_nqt))
175. plt.xlim(0, 200)
176. plt.xlabel('Normalized cone resistance nqt [-]')
177. plt.ylabel('pdf-normal distribution')
178. plt.title('The pdf of nqt in the middle column after removing the central CPT')
179.
180. plt.figure()
181. x_axis_nfr = np.linspace(min(min_middleC_nfr), max(max_middleC_nfr), 100)

```

```

182. plt.plot(x_axis_nfr, norm.pdf(x_axis_nfr, final_mean_middleC_nfr, final_std_middleC_nfr))
183. plt.xlim(0, 4)
184. plt.xlabel('Normalized friction ratio nfr [-]')
185. plt.ylabel('pdf-normal distribution')
186. plt.title('The pdf of nfr in the middle column after removing the central CPT')
187.
188. ##Read CPT81 which is the conducted CPT in the middle and compare
189. df81 = pd.read_excel('CPT81.xlsx')
190. depth81 = -df81.values[:, 0]
191. qt81 = df81.values[0:, 1]
192. fs81 = df81.values[:, 2]
193. sigv81 = df81.values[:, 5]
194. sigv_eff81 = df81.values[:, 6]
195. nqt81 = (qt81 - sigv81)/sigv_eff81
196. nfr81 = (fs81*100)/(qt81 - sigv81)
197. log_nqt81 = np.log(nqt81)
198. log_nfr81 = np.log(nfr81)
199. ##Remove some abnormal values
200. # nqt81 = nqt81[9:-1]
201. # nfr81 = nfr81[9:-1]
202. # depth81 = depth81[9:-1]
203.
204. #####The range of simulated results and real condition#####
205. plt.figure()
206. plt.plot(nqt81, depth81, label = 'measured')
207. plt.plot(max_middleC_nqt, depth81, label = 'max')
208. plt.plot(min_middleC_nqt, depth81, label = 'min')
209. plt.xlabel('normalized qt [-]')
210. plt.ylabel('depth [m]')
211. plt.legend()
212. plt.title('The measured CPT nqt and simulated boundaries')
213.
214. plt.figure()
215. plt.plot(nfr81, depth81, label = 'measured')
216. plt.plot(max_middleC_nfr, depth81, label = 'max')
217. plt.plot(min_middleC_nfr, depth81, label = 'min')
218. plt.xlabel('normalized fr [-]')
219. plt.ylabel('depth [m]')
220. plt.legend()
221. plt.title('The measured CPT nfr and simulated boundaries')

```